MASTERARBEIT / MASTER'S THESIS

Titel der Masterarbeit / Title of the Master's Thesis

„Elucidating the molecular mechanisms of prebiotic induced alterations in the gut microbiome“

verfasst von / submitted by

Deniz Inan BSc

angestrebter akademischer Grad / in partial fulfilment of the requirements for the degree of

Master of Science (MSc)

Wien, 2022 / Vienna, 2022

Studienkennzahl lt. Studienblatt / degree programme code as it appears on the student record sheet:	UA 066 834
Studienrichtung lt. Studienblatt / degree programme as it appears on the student record sheet:	Masterstudium Molekulare Biologie UG2002
Betreut von / Supervisor:	Univ.-Prof. David Berry, Privatdoz. PhD

Acknowledgments

I would like to express my appreciation to Univ.-Prof. David Berry for the opportunity to do my master's thesis under his supervision.

I would also like to cordially thank Hamid Rasoulimehrabani, MSc and Georgi Nikolov, MSc for their support and assistance in the lab.

Moreover, a special thanks goes to Dr. Alessandra Riva, who has been a great mentor from the start and shared all her knowledge with me.

I would also like to express my gratitude to my dearest friend Sophie Sandner and my boyfriend Fabian Loss. Sophie thank you for supporting me from the beginning of my studies here in Vienna and being there for me during stressful periods. Fabian thank you for always lifting me up and doing life together with me.

Last, I would like to thank my family, especially my mum Sezer Inan, who has always believed in me and encouraged me to reach my goals. Without the great people in my life, I wouldn't be at this point in my life.

Table of Content

Abstract

A broad spectrum of prebiotic compounds has been shown to stimulate the intestinal microbiome. Here we elucidated the effect of the candidate prebiotics xylooligosaccharides (XOS) and lactulose on individual bacteria of the human gut microbiome, along with providing methods for the investigation of prebiotic compounds. First, we analysed the metabolic activity in the presence of XOS and lactulose in human faecal samples of 6 different donors by applying Raman microspectroscopy together with Deuterium-isotope labelling, which is incorporated into cells during cellular, but mainly lipid biosynthesis. This revealed higher metabolic activity in the presence of XOS or lactulose in comparison to no amended samples for all donors. To identify single taxa which respond to XOS or lactulose we performed Raman activated cell sorting and cultivation. 16S rRNA gene sequencing of isolated strains revealed that taxa from the genus *Bifidobacterium* and *Collinsella* were able to utilize the compound XOS, as well as lactulose. Additionally, we were able to identify taxa from the genus *Lactococcus* as lactulose utilizer. Our findings also indicate actions of cross-feeding in the presence of lactulose. Potential secondary degraders may be members of the genus *Adlercreutzia, Bacteroides* and specific species of *Collinsella.*

1 Introduction

1.1 Introduction to the human gut microbiome

The human gastrointestinal tract (GIT) harbours a complex and dynamic population of microorganisms: “the gut microbiota”. The gut microbiota co-evolved with the host over thousands of years to form an intricate and mutually beneficial relationship. Presently over 1000 different microbial species that can reside in the human GIT are composed of all three domains of life: Bacteria, Archaea, and Eukarya[1]. The microenvironment in the gut favours the growth of bacteria from the phyla *Firmicutes, Bacteroidetes, Actinobacteria, Proteobacteria, Fusobacteria, Verrucomicrobia,* and *Cyanobacteria*[2]. Whereat four major phyla *Firmicutes, Bacteroidetes, Actinobacteria,* and *Proteobacteria* dominate and represent up to 97% of the total bacteria. The composition of the gut bacteria and its diversity is determined by a range of factors for example age, genetics, location, social behaviour, hygiene, and nutrition[3]. Although these factors cause variation in the microbiome composition of every individual, there are still distinctive compositional and functional features in the microbiome that appear across different life periods. The debate if microbial shifts like nutritional changes during infancy (breastfeeding to solid nutrition), hormonal changes during puberty, or maturation of the gastrointestinal tract during adulthood reflect secondary biological changes or if they are the root of physiological transitions during an individual’s lifespan is ongoing[4].

1.2 Acquisition of the human gut microbiome

The first moment of colonization is not clear as there are two theories: the sterile womb paradigm and the utero colonization hypothesis. The initial colonization from maternal to offspring in utero has been criticized because of the limitations to investigate the foetal microbiome and the high susceptibility of contamination and false positive results[5]. Overall this discussion is ongoing, and more evidence needs to be generated to fully understand the beginning of GIT colonization. What is known, is that the way of birth affects the first composition of the gut microbiome.

New-borns delivered via vaginal birth show an occurrence of *Lactobacillus and Prevotella spp*., whereas new-borns delivered via C-section show a predominance of *Staphylococcus, Corynebacterium and Propionibacterium spp.* resembling the microbial community of the skin[6–8]. Further development of the gut is influenced by nutrition of the infant as breast feeding and formula milk leads to the establishment of different bacteria phyla in the gut. Breast feeding supports the growth of mainly *Bifidobacterium* as it contains fats, proteins, immunoglobulins and human milk oligosaccharides (HMO)[9]. Furthermore, breast feeding contributes to the establishment of the ability to metabolize lactate and plant-derived glycans[10]. On the other hand, formula milk facilitates the growth of *Bacteroides* and *Clostridium* in higher levels and frequency than in breast milk fed infants[9]. The content of the breast milk shapes the microbiota which in response influences the impact of the microbes on the infant. A key effect of this is supporting the maturation of the immune system.

The next big shift in the colonization process happens during the introduction of solid foods and indigestible carbohydrates into the diet[10]. This leads to a dominance of *Bacteroidetes* and *Firmicutes* and a general enrichment of bacteria equipped with genes that encode for the metabolization of a large variety of carbohydrates, vitamin biosynthesis, and xenobiotic degradation[11,12]. Around the age of three the bacterial complexity and diversity resembles the one of adults. Although newer studies indicate a slower evolvement of the gut microbiome as children around the age of three show functional and taxonomic differences compared to the adult microbiome[13]. The life phase of adolescence is marked by the influx of sex hormones which is associated with gender specificity of the existing microbiome[4]. Summarized the functionalities and diversity of the microbiome enhances with age until establishment of an adult microbiome.

Bacteria colonize different parts of the human GIT with a different degree in density, which increases from the proximal to the distal gastrointestinal tract, harbouring the majority in the colon[14]. Starting with the stomach the density of residing bacteria accounts $<10^3$ CFU/ml. The small intestine (SI) consists of three parts the duodenum, jejunum, and ileum with the main function of digesting and absorbing foods and nutrients. As the microenvironment is distinct in the different parts of the SI also the bacterial density and diversity differ.

The microenvironment in the duodenum, characterized by oxygen, bile acids, pancreatic secretions, and antimicrobial agents limits the bacterial density to 10^{3-4} CFU/ml. Density increases already in the jejunum to 10^{3-7} CFU/ml supporting the growth of mostly Gram-positive aerobes and facultative anaerobes, followed by 10^{9} CFU/ml in the ileum favouring anaerobes and Gram-negative organisms in the distal part of the ileum[15,16]. The large intestine (LI), which is divided into the caecum and colon, is characterized by slower transit of food and anaerobic conditions. Therefore, water absorption and fermentation of undigested foods happen primarily in the LI with a bacterial density of 10^{12} CFU/ml[15,17]. In the LI the primary present bacteria phyla are *Bacteroidetes* and *Firmicutes*. The ratio of these two phyla is often consulted as a marker in health and diseases[18].

1.3 Functionalities of the gut microbiome

The gut microbiota has a critical influence on the health status of the host by contributing to different physiological processes like energy homeostasis, metabolism, gut epithelial health, immunologic activity, and neurodevelopment[19]. One key function is the metabolization of carbohydrates. The human gastro intestinal tract is not equipped with enough digestive enzymes to metabolise every carbohydrate. The human genome encodes 97 glycoside hydrolases (GHs) with eight of them involved in digestive processes, and further nine possibly linked to digestion[20]. For this reason, digestive processes are depended on the functions of the gut microbiota.

Dietary fibres like resistant starch, non-starch polysaccharides and oligosaccharides, also summarized under the term non-digestible carbohydrates (NDC), that cannot be digested and absorbed in the SI reach the LI where they undergo microbial breakdown and fermentation[21]. Since these polysaccharides differ in their structure and their glycosidic bonds linking the moieties, diverse enzymes are necessary for their breakdown[20]. The more complex the polysaccharide the more enzymes are required to metabolise these structures[22]. Gut bacteria are equipped with enzymes collectively called carbohydrate active enzymes (CAZymes, www.cazy.org)[23].

They metabolise the accessible carbohydrates into fermentable monosaccharides. CAZymes are categorised into four classes of glycosidases, glycoside hydrolase (173 families), glycosyltransferases (115 families), polysaccharide lyases (42 families), and carbohydrate esterases (20 families)[24]. Among members of each family the catalytic machinery, molecular mechanism, and stereochemical outcome is conserved, excluding some rare exceptions. The human gut microbiota devotes a vast part of its genome to CAZymes due to evolutionary processes and the competitive advantage these acquirements generate for them[20]. The breakdown of complex carbohydrates results to a majority in the generation of short chain fatty acids (SCFA), delivering approximately 10% of the energy budget of the host[20,25].

Many studies show that diet influences the diversity of the gut microbiota. For example, the Hadza hunter gatherers from Tanzania represent a community with a diet enriched in complex carbohydrates, which reflects the high diversity of their gut microbiota[26,27]. In contrast a diet high in fat and sucrose can provoke the disappearance of different beneficial taxa of the gut microbiota[26,28]. Hence, the fermentation of complex fibres and the generation of SCFA contribute to the health status of the host. The three major SCFA generated are acetate (60%), butyrate (15%), and propionate (25%)[26,29–31]. If the fermentable fibre source is limited some bacterial species can also utilize amino acids, proteins, and dietary fats for the production of SCFA, but in less quantum.[26,32] All three major SCFAs are produced by different pathways and microbes. Acetate is mainly formed from pyruvate via acetyl-CoA or via the Wood-Ljungdahl pathway, butyrate from lactate via the butyryl-CoA: acetate CoA-transferase or phoshotransbutyrylase/butyrate kinase route and for the production of propionate succinate is metabolized via the succinate pathway[26,33–36]. Also, propionate can be formed from the substrate's acrylate with lactate via the acrylate pathway or from deoxyhexose via the propanediol pathway[26,36,37]. The concentration of SCFA ranges in the GIT from highest levels in the cecum and proximal colon (70-140 mmol/L) and lower levels towards the distal colon (20-70 mmol/L)[26,29,38]. Furthermore, the concentration of SCFA is affected by different factors such as the pH in the gut, the composition of the host microbiota, the type and concentration of fermentable substrates, and the capability to absorb the SCFA from the intestine[39,40].

Dependent on the absorption and the local concentration, SCFA exert distinct functions and play a role in many physiological processes. In the colon the most abundant SCFA is butyrate, as it is the favoured energy source of colonocytes, whereas other SCFAs drain into the portal vein[26,29]. In the peripheral circulation acetate is present in high concentrations and is able to cross the blood-brain barrier, while propionate is less abundant in the periphery, as it is metabolized in the liver[26,29,41]. Although butyrate and propionate are only present in low concentrations in the peripheral circulation, they affect peripheral organs indirectly by influencing hormonal and neuronal signalling[26].

Due to the physiological environment and the pH range from 5.5 to 6.7 SCFA exist mostly in the ionised form and transporters are required for their absorption[29,42,43]. Further signalling happens presumably through G-protein coupled receptors (GPCR), which are GPR41 (FFAR3), GP342, GPR43 (FFAR2), GPR109a (HCAR2), GPR164 (OR51E1) and OR51E2[43]. SCFAs act on proliferation and differentiation of cells. Butyrate is highly present in the gut lumen and therefore is the primary energy source of intestinal epithelial cells (IEC) where it is oxidised in the mitochondria via β-oxidation[43–46]. Moreover, it is able to repress the expansion of transformed cells, due to the phenomenon of the Warburg effect[43,47,48]. SCFA have an important role in supporting epithelial barrier function through different mechanisms. Specifically, butyrate influences the epithelial barrier function through co-ordinated regulation of tight junction proteins (TJP) and by reducing the permeability via the transcription factor, Hypoxia-inducible-factor HIF[49,50].

In addition, SCFA modulate the mucus layer thickness and as well enhance barrier function by regulating the secretion of antimicrobial peptides by the gut epithelial cells[51–54]. There is the importance of keeping the intestinal barrier intact, as increased permeability is associated with translocation of bacteria and their cell wall components, which can initiate an inflammatory cascade and has been linked to obesity and insulin resistance[49,55]. Besides the IEC, SCFA also stimulate enteroendocrine cells (EEC) which leads to the secretion of hormones like glucagon-like peptide (GLP)-1 and peptide-tyrosine-tyrosine (PYY) affecting satiety and glucose homeostasis[43,51,56–59].

Another prime role of these SCFA is the interaction with the immune system, supporting the maintenance of a favourable environment for commensal bacteria and controlling the growth of pathogens. SCFA show an anti-inflammatory effect by up-regulating anti-inflammatory and down-regulating pro-inflammatory cytokines by various mechanisms facilitating the mucosal homeostasis. These mechanisms include for example signalling pathways like nuclear factor kappa-light-chain-enhancer of activated B cells (NK-κB), extracellular signal-regulated kinase (ERK) and p38 mitogen-activated protein kinase (MAPK)[60,61]. Also, a key mechanism for the interaction with the immune system is the inhibition of histone deacetylation (HDAc) by SCFA in specific inflammatory signalling pathways as well as on an epigenetic level[60,62–64]. Metagenomic approaches allowed the characterization of bacteria responsible for SCFA production. Various bacteria are equipped with pathways to generate the SCFA acetate, whereas the ability to produce propionate, butyrate and lactate is more highly conserved and substrate specific[49,65].

The diverse members of the gut community do not act as single microbes, but they indeed interact with other members. This is essential for the diversity and stability of this complex ecosystem. One essential way of interaction is cross-feeding, which describes the metabolic exchange between the gut microbiota[51]. In difference to true cooperation, the production of metabolites does not require additional energy as these molecules are the by-products or the result of macromolecule degradation[66,67]. For example, the well-studied prebiotic inulin, a fructose polymer is metabolized by several members of the gut microbiota like *Bifidobacterium, Roseburia, Bacteroides, and Lactobacillus*[66,68]. The inulin derived molecules lactate and acetate are then converted into butyrate by e.g. *Faecalibacterium prausnitzii*[66,69]. Not only SCFA are involved in this exchange but also molecules such as amino acids and vitamins. Taken together further studies are necessary to fully understand the extent of microbial communication in the gut and the relevance for health and disease in the host.

1.4 Defining prebiotics

The concept of prebiotics evolved over the last decades[70]. In 2017 the International Scientific Association of Probiotics and Prebiotics (ISAPP) redefined the definition of prebiotics as selectively fermented components, which allow specific changes in the composition and/or activity of microorganisms in the gastrointestinal tract and have a beneficial effect on host's health and wellbeing. Further criteria have to be fulfilled like resistance to gastric acid and hydrolysis by mammalian enzymes, gastrointestinal absorption and the ability to be utilized by the intestinal microbiota and their stimulation. Predominantly, prebiotics are carbohydrate-based compounds but substances like polyphenols and polyunsaturated fatty acids have been in discussion to exert prebiotic effects as well[71]. Currently the most studied prebiotics are fructans like fructo-oligosaccharides (FOS), as well as galactans such as galacto-oligosaccharides (GOS)[72.]. Fructans are composed mostly of chains of fructose units with a glucose molecule and can be subdivided into short-chain FOS, nystose, ketose, and longer chain inulin[73,74]. GOS can also be further categorized into α-linked and β-linked GOS of which α-linked molecules have been found to stimulate the growth of a wider range of gut bacteria species[73,75,76].

Prebiotic compounds are fermented by specific groups of microorganisms into mostly SCFA affecting the composition of the intestinal microbiota and their metabolism. This happens through the modulation of lipid metabolism, enhanced calcium absorption, effect on the immune system, and modification of bowel function[77]. Natural occurring prebiotic substances can be found in various plant-based foods such as vegetables, fruits, and cereals. A balanced European diet can provide 3-11g of natural prebiotics per day[78]. Prebiotics are also produced on an industrial scale through the hydrolyzation of polysaccharide or enzymatic reactions from lower molecular weight sugars[72,78].

1.5 Candidate prebiotic compounds xylooligosaccharides and lactulose

In our study, we investigated the prebiotic candidates XOS and lactulose, as there are limited studies on these compounds. XOS are carbohydrate oligomers, which consist of xylose residues linked through β-(1,4)-xylosidic bonds[79]. They naturally occur in foods like fruits, vegetables, milk, honey, and bamboo shoot and can additionally be commercially produced through a range of chemical methods like direct enzymatic hydrolyzation[80,81]. For the metabolization of XOS the gut bacteria have to be equipped with specific enzymes, one being endo-xylanase which breaks down the β-(1,4)-xylosidic bonds of the backbone into shorter fragments and the other being β-xylosidase, which removes xylose units from the non-reducing terminal of the xylooligosaccharides[82,83]. β-xylosidases represent key enzymes in the breakdown process of XOS as the xylose units generated by it can further be metabolized in the isomerase pathway. It is further converted into xylulose phosphate, which subsequently enters the pentose phosphate pathway (PPP)[84]. Based on current information β-xylosidases with activity on natural substrates belong to 8 families of GH, namely GH 3, 5, 30, 39, 43, 51, 52, and 120 (CAZymes, www.cazy.org)[24,83].

On the contrary, lactulose is a synthetic disaccharide which consists of galactose and fructose monosaccharide units which are linked through β-(1,4)-glycosidic bonds. Industrially it is produced through the isomerization of lactose[85]. In 1957 it has been shown that the genus *Bifidobacterium* increased after the administration of lactulose in infants determining clinical interest in the compound[86,87]. Since then lactulose has been used as an osmotic laxative (starting from 10g/day) to treat constipation in adults and children. Furthermore, it is used as a detoxifying agent for the treatment of hepatic encephalopathy (HE) in adults[40,85,88]. For the application of lactulose as prebiotic low doses are applicable. Possible enzymes necessary for the breakdown of lactulose by the gut bacteria are α-galactosidase and β-galactosidase, which belong to the class of GH as well, specifically to the families GH 2 and GH 42[89].

1.6 Dysbiosis of the gut microbiome

The complex and dynamic ecosystem in the gut is affected by diet, environment, medical interventions, and diseases. Alteration in the gut microbiota and the change of relative abundance between the different bacteria phyla, which is defined as dysbiosis, is correlated to inflammation, metabolic syndromes, leaky gut, and other chronic inflammatory diseases like inflammatory bowel diseases including ulcerative colitis and Crohn's disease, autoimmune disease and neurological disorders[3,90,91]. Different factors contribute to the state of dysbiosis in the gut microbiome. Diet is a major element as an excess supply of nutrients and a high fat diet lead to metabolic disorders such as obesity, which is characterized by decreased microbial diversity[92]. An over-representation of *Firmicutes* has been determined in obese mice[93,94], as well as in humans[95,96]. In addition, a lower ratio of *Bacteroidetes* to *Firmicutes* results in a higher release of lipopolysaccharides (LPS) into the circulation, which as consequence facilitates a state of chronic low-grade inflammation in obesity[91,97].

As the gut microbiome is linked to the central nervous system (CNS) via the bidirectional gut-brain axis, stress may influence the composition of the microbiome. This was for example demonstrated via a model of social disruption among adult mice, which resulted in substantial changes in the gut microbiota. In these experiments, the social disruption was initiated by placing an aggressive male mouse into the resident mice cage for 2h. In comparison to the control group of mice, *Bacteroides spp*. decreased, whereas *Clostridium spp*. increased in the relative abundance in the stress-induced mice[98]. The mechanisms by which stress affects the microbiome are unclear but the concentration of noradrenalin in the gut lumen may contribute to the changes in the microbial community in the gut, as it can alter gene expression in some bacteria[99,100]. In human studies it was described that different kinds of stress like perceived stress[101], early life stress[102], adverse childhood experiences (ACEs)[103] and *in utero* stress[104] alter the microbial composition and/or diversity in the gut[105]. It is clear that understanding this complex relationship of the gut-brain axis, especially in humans is still a challenge, hence more studies are needed to explore these dynamics.

Other factors that can affect the microbiome are antibiotics and other medications. Antibiotic treatment reduces the overall diversity of the gut microbiome including the loss of important taxa. Consequently, this shifts metabolic processes in the gut, increases gut susceptibility to colonization and stimulates the development of bacterial antibiotic resistance[106,107]. In adults, an increased prevalence of *Enterobacteriaceae* and other pathobionts, and a decrease in *Bifidobacterium* and butyrate-producing species was observed after the administration of meropenem, gentamicin and vancomycin. Antibiotic treatment can lead to the overgrowth of pathobionts like the toxigenic *C. difficile*[106,108]. It is important to note that the effect of antibiotics on the gut microbiome depend on the type and combination of antibiotics, the mode of administration and duration of treatment[109]. Also, the administration of commonly used medications like aspirin, ibuprofen and naproxen, when taken over longer periods of time as well as proton pump inhibitors (PPI) can modify the composition of the gut microbiome[110]. PPI increase the gastric pH, which impairs the intestinal barrier and further can interfere with phosphatase activity and local electrolyte homeostasis[111,112]. Diet, stress, antibiotics and other medications are just some of the factors to mention that can influence the complex ecosystem of the gut microbiome.

1.7 Restoring homeostasis in the gut

One way to help restore the homeostasis in the gut is by the administration of prebiotics. As mentioned earlier the fermentation of prebiotic compounds generates SCFAs, which subsequently affect the health status of the host. The emerging prebiotic XOS promotes the growth of *Bifidobacterium* and *Lactobacillus*, increasing SCFA production in the gut[113]. In pre-diabetic patients XOS was able to enhance insulin sensitivity[114]. Fei et. al demonstrated that the administration of XOS in high fat diet (HFD) mice alleviated the effects of HFD including body and organ gain as well as some systemic chronic low-grade inflammation[115]. Also, for the candidate prebiotic lactulose studies demonstrated the positive effect on the host metabolism. The main SCFA produced by the fermentation of lactulose is acetate and through cross feeding other members of the gut bacteria produce butyrate[40,116–119]. These SCFA help to lower luminal pH, which helps to prevent pathogen growth and infection[40,117,120]. Moreover, the lowered luminal pH may contribute to the enhanced absorptions of minerals from the gut[40,121].

Additionally, lactulose may play a role in the treatment and prevention of diabetes as the produced SCFA support mucosal cells, enhance hepatic glycogenesis and lipogenesis and reduce secondary bile acids, which are elevated in Type 1 and Type 2 diabetes[122–124]. A reduced secondary bile acid profile facilitates a protective effect on pancreatic β −cells and reserves systemic insulin load[122,125].

Prebiotics can also be administrated together with probiotics, which is then described as synbiotic. The Food and Drug Administration (FDA) and the World Health Organization (WHO) defined probiotics as “live microorganisms which when administrated in adequate amounts confer a health benefit on the host”. Probiotic effects are strain dependent and probiotic products can contain either a single strain or a mixture of strains. Typical strains found in probiotic products are *Lactobacillus rhamnosus*, *Lactobacillus reuteri*, *Bifidobacterium strains*, certain strains of *Lactobacillus casei*, and *Bacillus coagulans*[126]. The International Scientific Association for Probiotics and Prebiotics has updated the concept of synbiotics by a panel of experts, differentiating synbiotics into complementary and synergistic types. Complementary describes synbiotics, which consist of probiotics and prebiotics that together confer one or more health benefits but do not require co-dependent functions. A synergistic symbiotic contains substrate(s) that are selectively metabolized by co-administrated microorganism(s)[127]. Different randomized controlled trials (RCTs) explored the beneficial effects of synbiotics in various populations, from healthy individuals to those with acute and chronic diseases. In any case, the selective utilization by either endogenous microbiota or co-administered microorganisms must be given. Formulation with the microorganism of the genera *Lactobacillus*, *Bifidobacterium,* and *Streptococcus* in combination with the prebiotic compounds galacto-oligosaccharides (GOS), fructo-oligosaccharides (FOS) and inulin in different concentration have been investigated[128,129]. For example, in an RCT study of diabetic patients undergoing haemodialysis, participants received a synbiotic capsule containing *Lactobacillus acidophilus*, *Lactobacillus casei,* and *Bifidobacterium bifidum* (2 x 109 CFU/day each) plus 0.8g/day inulin for 12 weeks. Synbiotic supplementation resulted in improvement of glycaemic control and biomarkers of inflammation and oxidative stress but did not significantly affect lipid profiles of patients[130].

1.8 Applied study techniques

1.8.1 Raman microspectroscopy

Raman microspectroscopy is a non-destructive vibrational spectroscopic method that allows obtaining information about the molecular composition of samples on microbial single cell level. It can further be combined with fluorescence staining and epifluorescence microscopy and radioactive- or stable-isotope labelling. The method is based on the following principle: a sample is illuminated with monochromatic light generated by a laser, some of the light photons are transmitted or absorbed, while other photons are scattered after the interaction with molecules of the sample. It can be differentiated between different types of scattering, Rayleigh scattering is when the scattered photons and the incident photons have the same energy and the excited molecule returns to its vibrational ground state, emitting photons with the same wavelength. Some of the scattered photons do not return to their vibrational ground state but rather to the first excited vibrational state, which is described as Stokes scattering. If a molecule is already situated in the first excited vibrational level, gets excited to a virtual energy level and returns to the vibrational ground state it is called anti-Stokes scattering[131].

In Raman microspectroscopy, Stokes scattering of photons is normally measured, as it occurs more frequently than anti-Stoke scattering. Depending on the molecule, different scattering of the photon will occur with different wavelengths, which can be seen as a band in the Raman spectrum. This allows the identification of several compound classes of a microbial cell. Some molecules show a specific peak in the Raman spectrum like phenylalanine or cytochrome C. The intensity of a Raman band in the spectrum is influenced by the excitation wavelength, the power of the laser, the temperature, the polarizability of the molecule, and the concentration of the Raman active molecule. The higher the Raman wave number ($(\lambda_0^{-1} - \lambda^{-1}) \times 10^7$) of a certain band, the lower the energy and the higher the wavelength of the Stokes scattered photon[131].

1.8.2 Determining metabolic activity using stable isotope-labelling

To understand complex metabolic processes like complex carbohydrate degradation in human gut bacteria, one can utilize a combination of Raman microspectroscopy and stable isotope-labelling with heavy water D_2O. This approach allows analysing metabolic active cells in the presence of specific compounds. During metabolic processes, the deuterium from the heavy water is incorporated into the biomass of cells, mostly into lipids during lipid biosynthesis but to some extent also into nucleic acids, proteins, and carbohydrates. This results in the formation of carbon-deuterium (C-D) bonds instead of carbon-hydrogen bonds (C-H), which is detectable as a specific peak in the Raman spectrum of a single cell between 2040 cm^{-1} and 2300 cm^{-1}.This peak appears in metabolic active microbes and cells, which do not show a detectable peak in this region of the Raman spectrum, are considered as inactive cells. The deuterium also does not interfere with the growth of the cells and shows no toxic effect, when incubated with concentrations up to 50% of D_2O. Additionally, the method is non-destructive and the fixation of cells is not a requirement[132].

1.8.3 Raman activated cell sorting

Raman activated cell sorting (RACS) is a relatively new method for sorting and separating single cells from complex communities. RACS combines Raman spectroscopy with a fully automated optofluidic platform that allows the targeting of stable isotope labelled cells. The approach can be applied to bacterial, archaeal, and potentially eukaryotic cells and analyses up to 200-500 cells/h[133]. Cells in the microfluidic cell isolation system move through the stable flow in the system to the detection point, where a single cell randomly is captured by the optical tweezer for the evaluation of the Raman spectrum based on the stable isotope labelling. The labelling status of the cell determines if the cell is released into the collection or the waste outlet of the system[133].

In our study, we utilized the stable isotope deuterium for the labelling of cells to sort active and living single microbial cells from the complex gut microbiome. For this system, two indicator parameters were established to represent the cells in the sorting process. The 'cell index' P_c determines cells present in the optical tweezer computed from the magnitude of the Raman signal in the spectrum region between 1620-1670 cm^{-1} and the integrated intensity I ($P_c = \frac{I_{1,620-1,670}}{I_{fluid,1,620-1,670}}$). This specific region was chosen as it is largely unaffected by the Raman spectrum of used materials polydimethylsiloxane (PDMS) and glass. On the other hand, the 'labelling index' P_L describes a captured cell, resulting from the deuterium status of the single cell. It is determined by the comparison of the region of the deuterium peak in the Raman spectrum 2,040-2,300 cm^{-1} (integrated intensity: $I_{2,040\text{-}2,300}$) to the region between 1,850-1,900 cm^{-1} (integrated intensity: $I_{1,850\text{-}1,900}$) ($P_L = \frac{I_{2,040-2,300}}{I_{1,850-1,900}}$)[133]. Lee et al. already demonstrated in their study the applicability of this method for model bacteria from different habitats with high sorting accuracy, throughput, and compatibility with cultivation.

2 Material and Methods

Previous work has been conducted by Aida Kadunic within her master's thesis applying the same methods to investigate the effects of the prebiotic compounds XOS and lactulose on the human gut microbiome[134].

The study was conducted in accordance with the University of Vienna ethics committee (reverence number 00161). Each donor was informed about the study and signed an informed consent form.

2.1 Experimental design

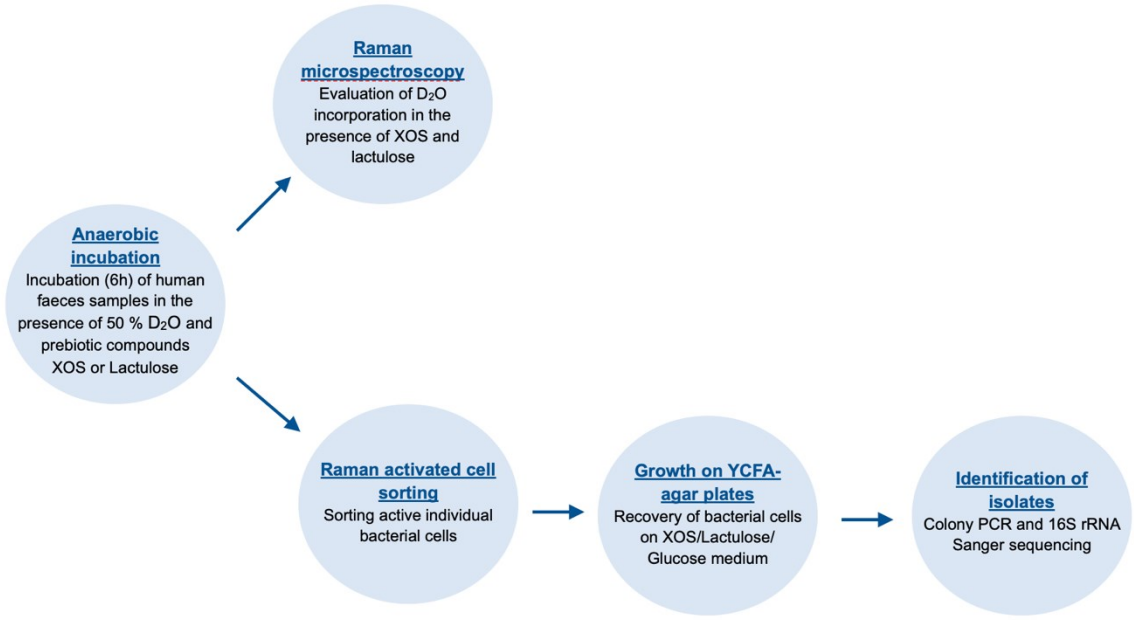

Figure 1 Description of experimental design.

2.2 Sample collection

Fresh faecal samples were collected from six different healthy donors (3 male and 3 females; BMI: mean $\pm$ sd: 23.3 $\pm$ 5.0)) with five being on an omnivore diet and one subject being vegetarian. None of the subjects was taking antibiotics, pre- or probiotics six months previous to sample collection. For the collection process, every subject was given an anaerobic jar (Thermo Fisher Scientific, MA, USA) with an anaerobic gas pack (Thermo Fisher Scientific, MA, USA) and a faecal collection tube (Sarstedt, Germany).

2.3 Anaerobic incubation

Incubations were processed in the anaerobic tent (85% N_2, 10% CO_2, 5% H_2). Therefore 1 g of fresh faecal sample was resuspended in 10 ml of phosphate-buffered saline (2 x PBS) and homogenized through vortexing for 2 – 4 minutes. The supernatant was transferred to a 50 ml falcon tube and diluted 1:5 by adding 2 x PBS. The substrates XOS, lactulose, glucose, galactose, fructose, and xylose were dissolved in 100 % D_2O with a final concentration of 2.5 mg/ml. In glass vials, 2 ml of the substrate solution with D_2O (final concentration of D_2O: 50%) and 2 ml of faecal suspension were incubated at 37 °C for 6 hours. No amendment samples plus D_2O were used as negative controls. At timepoints T0 (0 hours) and T6 (6 hours) 1 ml was collected for nucleic acid extraction and stored at -80 °C, 1 ml was fixed in 1:1 EtOH (96 %) and stored at -20 °C and a further 1 ml was stored in 20% glycerol in crimp sealed vials with rubber stoppers at -80 °C. These glycerol stocks were used for Raman activated cell sorting.

2.4 Raman microspectroscopy

Raman microspectroscopy was performed for stool samples previously incubated with XOS or lactulose for 6 hours (T6). No amendment control was used as negative control of the measurements. Therefore, for the XOS amended samples glycerol stocks were used and for the lactulose amended samples, as well as for the no amended samples the EtOH fixed. For sample preparation, 1.5 μl was directly spotted on an aluminium coated slide (A1136; EMF Corporatio, USA) and incubated at 30 °C to dry. Afterwards, the slide was dipped into Milli Q water (Millipore, MA, USA) to remove traces of buffer components and put back into the incubator at 30 °C for a second drying step. To acquire microbial single cell spectra a confocal Raman microspectroscope (LabRAM HR800, Horiba Scientific, France) equipped with a 532 nm neodymium-yttrium aluminium garnet laser and 300 grooves/mm diffraction grating was utilized. Raman spectra were generated with the software Labspec 6 (Horiba Scientific, France) in the range of 400-3200 cm^{-1} in the Raman spectrum. The settings for the acquisition time and the accumulations were as followed: 10 seconds and accumulation at 5. For each sample, 30 – 40 single microbial cell measurements were collected.

The threshold was determined by calculating the mean + 3 times the standard deviation (sd) of CD percentage in randomly selected cells from a stool sample incubated without addition of D_2O (water control). The evaluation of deuterium incorporation and therefore the formation of chemical bonds with carbohydrates (C-D bonds 2,040 – 2,300 cm^{-1}) was calculated using the integration of the specific region for C-D bonds with the single cell analysis and testing tool for Raman microspectroscopy Scattr (http://shiny.csb.univie.ac.at:3838/scattr/) with the following settings: alignment none, baselining polynomial at 3, normalization total spectrum.

2.5 Raman activated cell sorting

Raman activated cell sorting was performed following the design and working protocol designed by Lee et. al.[133] with modifications to the sample preparation regarding rpm and time of centrifugation.

2.5.1 Fabrication of microfluidic chambers for RACS

For the fabrication of microfluidic chambers polydimethylsiloxane (PDMS) was used, mixing the base elastomer (Sylgard 184™, Dow corning, Michigan, USA) and current agent (Sylgard 184™, Dow corning, Michigan, USA) in a ratio of 10:1 with the resulting weight of 10 g to receive a 1 mm thin layer of PDMS. The mixture was poured into an empty petri dish with the fixed master mould in it. The master mould is the pre-engineered pattern for the fabrication of the microfluidic device. Additionally, a second mixture of elastomer and current agent in a ratio of 10:1 with the resulting weight of 70g, was poured into another petri dish to receive a 5 mm thick layer of PDMS for the assembly of bricks. Both petri dishes were incubated at 75 °C for 60 minutes for polymerization. The microfluidic chips were cut out using blunt-end tweezers. For each chip, two bricks, cut from the 5 mm thick PDMS, were mounted onto the chip using a corona treater (Electro-technic products, Illinois, USA) one brick covering the inlet port and the other the outlet port. To allow chemical linkage the assembly was incubated at 75 °C for 60 minutes. Afterwards using a puncher (Ø 0.75 mm, WellTech, Taiwan) the ports were exposed making it possible to attach the tubing systems for RACS. The fabrication of the chambers was finalised by attaching the PDMS chip onto a high precision glass coverslip (60 x 24 x 0.17 mm, Paul Marienfeld, Germany) using the corona treater. The final assembly was incubated at 75 °C for 60 minutes and afterwards was ready to use.

2.5.2 Sample preparation

Living cells were sorted from the stool samples previously incubated with the prebiotic compound XOS or lactulose and in the presence of D_2O for 6 hours and stored in 20% glycerol on - 80 °C. The samples were thawed and 300 μl of the sample was centrifuged at 10.000 rpm (revolutions per minute) for 10 minutes until a pellet was formed. This was followed by two washing steps using 250 ml of 0.3 M PBS/glycerol and centrifugation at 7.000 rpm for 7 minutes. Afterwards, the sample was resuspended in 500 μl of 0.3 M Glycerol/PBS and introduced into a 500 ml Hamilton syringe (Hamilton, Nevada, USA). All preparations were done in the anaerobic tent, except the introduction of sample into the syringe.

2.5.3 Sorting process

RACS is an automated optofluidic platform consisting of single cell Raman detection instrument (532 nm laser at 90 mV, Horiba Scientific, Japan), an optical tweezer (1,064 nm Nd:YAG laser at 500 mV), syringe system (neMESYS 290 N, Cetoni, Germany) and a cell isolation microfluidic system. Calibration prior to every sorting was done using a silicon crystal showing a peak at 520 cm^{-1} in the Raman spectrum. The capillary syringe system brings two flows into the microfluidic system the sample flow through a 500 ml Hamilton syringe (Hamilton, Nevada, USA) and the sheath flow (1 x PBS/glycerol) through a 1 ml Hamilton syringe (Hamilton, Nevada, USA). Furthermore, the system includes two outlet flows one connected to a 1 ml syringe (BRAUN, Hessen, Germany) for the collection of captured single cells the other to a 1.5 ml Eppendorf tube (Eppendorf, Hamburg, Germany) collecting unlabelled single cells (waste outlet). The syringe system was controlled using the software Nemesys (Cetoni, Germany). To start the flow in the microfluidic chamber, prior to every sorting the flow was set in the following order collection channel, sheath fluid, and last sample according to the flow rates 2,7,5 μl/min. The design of the microfluidic chamber implements the cell flow on one side of the channel allowing the traverse to the analysing region and exit through the waste outlet by default. Single cells are captured, and their Raman spectrum is measured by the optical tweezer leading to a translocation of the deuterium labelled single cell to the release region into the collection outlet.

This process is fully automated by a software based on the K-means algorithm in Matlab 4.2. (Mathworks, USA) working through two main indicator parameters ‘cell index P_c’ and ‘label index P_L’. P_c is the parameter to describe the detection of a cell in the optical tweezer and in our case P_L for the identification of the deuterium-labelling status. The threshold was configurated using one of the human faecal samples amended with glucose and H_2O. Thus, the threshold value for P_L = 5,8 and P_c = 1,1 was determined based on the mean + 3 SD. Flow rates were decreased starting the sorting in the order sample, sheath fluid, collection channel according to the flow rates 0.06, 0.25 and - 0.1 μl/min to allow a stable flow and a passing through the waste outlet by default. A detailed material list can be found in table 8. After 60-90 minutes the sorting was stopped and 100 μl from the collection tube was collected.

2.5.4 Culturing of active fraction

Immediately after the sorting and collection, the cells were introduced into the anaerobic tent. 100 μl of the collected cells were plated on Yeast Casitone Fatty Acids (YCFA)-glucose plate to recover the single cells and incubated in the anaerobic tent at 37 °C. As control 100 μl of the used PBS/glycerol sheath fluid was plated on a YCFA-glucose plate to control for possible contamination in any case. After the growth of the single colonies, a single streak of every colony was performed on YCFA-glucose and incubated again at 37 °C until single colonies formed. Afterwards, the single colonies were streaked on YCFA amended with XOS or lactulose depending on which prebiotic compound the sample was incubated first.

2.6 Colony PCR and 16S rRNA Sanger sequencing

For the identification of bacteria colonies grown on YCFA plus XOS or lactulose agar plates, colony PCR was performed. The master mix was prepared in the PCR hood accordingly to table 1. The inoculation of chosen bacteria colonies was operated in the anaerobic tent. To amplify the 16S rRNA gene the primers 616V (5'-AGA GTT TGA TYM TGG CTC AG- 3') and 1492R (5'-GGT TAC CTT GTT ACG ACT T-3') were used with the amplification cycles: 95 °C for 3 min, 30 cycles at 95 °C for 30 s, 72 °C for 1.5 min and a final elongation phase at 72 °C for 10 min.

The PCR products were purified using the InnuPREP PCRpure Kit (Analytik Jena, Germany) according to the manufacturer's protocol. The concentration (ng/μl) was measured for each of the amplicons by nanodrop (Thermo Fisher Scientific, MA, USA) and afterwards sent for sanger sequencing at Microsynth AG (Vienna, Austria).

Table 1. Detailed description of master mix for 16S rRNA colony PCR.

Master mix compounds for one reaction	1x in μl
10x Green DreamTaq buffer including 20 μm $MgCl_2$ (Thermo Fisher Scientific)	5
dNTPs 2mM (Thermo Fisher Scientific)	5
Primer forward 616V, 50 μM (Thermo Fisher Scientific)	1
Primer reversed 1492R, 50 μM (Thermo Fisher Scientific)	1
BSA 20mg/ml (Thermo Fisher Scientific)	0,5
Dream Taq Polymerase 5U/μl (Thermo Fisher Scientific)	0,5
H_2O PCR grade (Thermo Fisher Scientific)	37
Total volume	50

2.7 16S rRNA gene analysis

Microsynth AG 16S rRNA gene sequence results of forward primer and reverse primer sequence were analysed with the program 4Peaks 1.8 (Nucleobytes, Amsterdam, Netherlands). With the same program, the start and end of the sequence was trimmed to exclude poor peaks. The forward and reverse primer 16S rRNA sequences were aligned with the program Serial Cloner 2.6. This was done for all sequences of sorted single cells of the different donors. Last the aligned 16S rRNA sequence was checked for chimera with the online tool DECIPHER[135]. To identify which bacterial taxa correspond to each RACS sorted strain, the aligned 16S rRNA sequences were analysed using the online tool NCBI Blast, finding the best match by comparing it to the database (average best match n ≥96%)[136]. Sequences of the isolated strains have been submitted to GenBank under the accession numbers OP183499-OP183547 (XOS) and OP179799-OP179820, OP179823, OP179824, OP179826-OP179849 (lactulose).

2.8 Generation of phylogenetic trees

Representative strains of all donors were selected for phylogenetic analysis based on the length of the sequence (≥ 650 bp). Sequences were aligned with the web resource silva (Max Planck Institute for Marine Microbiology and Jacobs University, Bremen, Germany), referring the sequences to their database of rRNA gene sequences of the domains Bacteria, Archaea, Eukaryota[137–139]. Afterwards, the phylogenetic trees were generated with a maximum likelihood algorithm inclusively bootstrapping in IQtree and rooted at midpoint. The best-fit model determined by the model finder for strains isolated from XOS amended samples was TN+F+G4 and for lactulose K2P+G4[140]. The phylogenetic trees for the representative strains were then visualized with the online tool iTOL[141].

3 Results

3.1 Detection of D_2O incorporation in the presence of XOS and lactulose

The Raman single cell measurements were taken for all samples at T6 and showed incorporation of deuterium for samples amended with XOS as well as lactulose. For that reason, correlating the incorporation of D_2O and the formation of C-D bonds to the metabolic activity of the bacteria in the amended samples. An example for this is shown in figure 2. The samples with the prebiotic candidate compound XOS or lactulose showed deuterium incorporation in the Raman spectrum (2,040 – 2,300 cm^{-1}) in comparison to the no amendment controls. On average 35-40 single cell measurements were taken for each donor. Figures 3 and 4 display the CD percentage of all the single cell measurements for each sample amended with XOS or lactulose compared to no amendment. In our experiment the threshold was calculated as ~2,56. In the presence of XOS, the single cell measurements of donor 2 showed the highest average of CD percentage 7.69±3.45%, whereas donor 4 the lowest 5.69±3.97%. For samples incubated with lactulose, the single cell measurements for donor 3 revealed the highest average of CD percentage of 10.18±3.45%, whereas donor 4 the lowest 3.53±2.43%. An overview of the average CD percentage for each donor is shown in table 2.

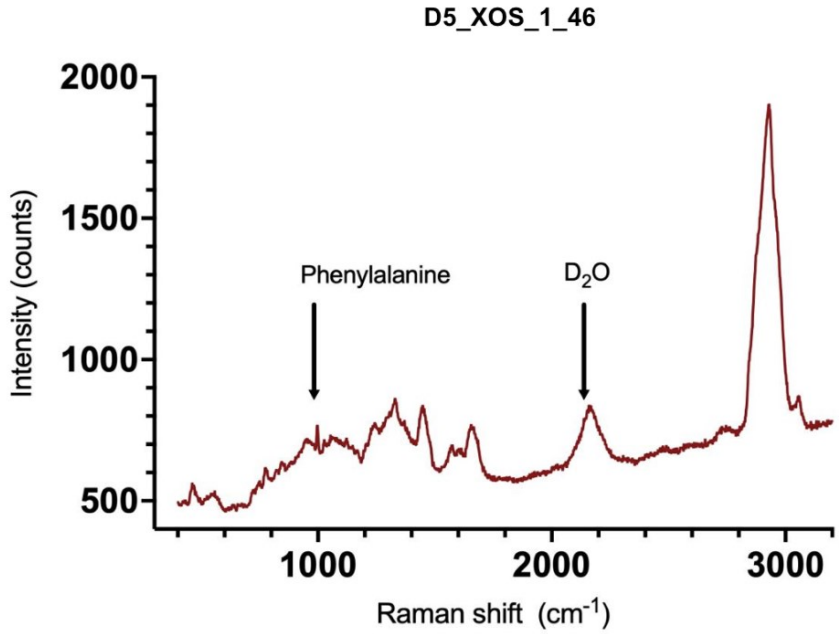

Figure 2. Example of D_2O peak (2,040 – 2,300 cm^{-1}) in the Raman spectrum.

A Raman spectrum of sample donor 5 amended with XOS - single cell measurement number 46 is shown. Detectable peak in the region 2,040 – 2,300 cm^{-1} of the Raman spectrum. Identification as bacterial cell by phenylalanine (1000 cm-1) and carbohydrate peak.

Table 2. Overview of average CD% of samples from Donor 1-5 (D1-5)

Average CD% + sd of samples amended with XOS and lactulose for each donor.

Donor	Average CD% + sd with XOS	Average CD% + sd with lactulose
D1	6.80±4.54	4.35±3.02
D2	7.69±3.45	4.06±2.68
D3	7.00±3.36	10.18±3.45
D4	5.69±3.97	3.53±2.43
D5	5.97±5.38	5.85±2.16
D6	7.27±3.92	4.73± 3.47

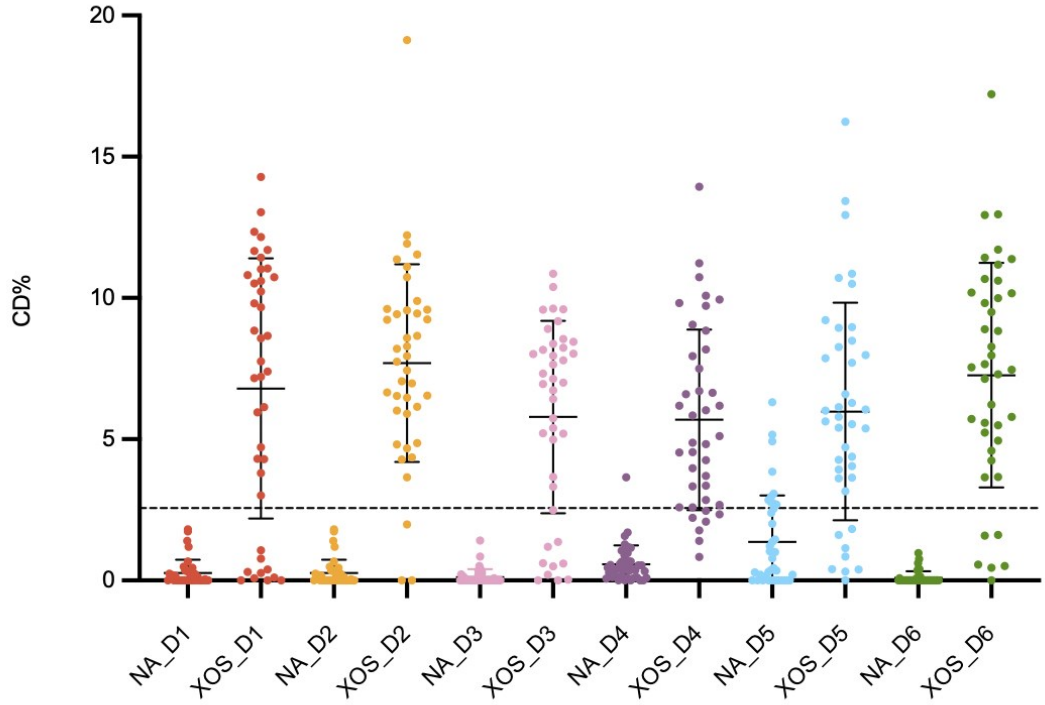

Figure 3. Comparison of all CD percentages of single cell measurements for donor 1-5 (D1-5) of XOS amended and no amended samples (NA). *The x-axis represents D1-5 samples divided into samples incubated in the presence of XOS or NA. Y-axis describes CD%. Calculations were generated by the testing tool Scattr with the following settings: alignment none, baselining polynomial at 3, normalization total spectrum. Each coloured dot represents the CD% of a Raman measurement for a single cell. The dashed line marks the threshold, which was determined by calculating the mean + 3 sd of the measurements of sample 3 amended with glucose and no D_2O. Threshold: ~2,56.*

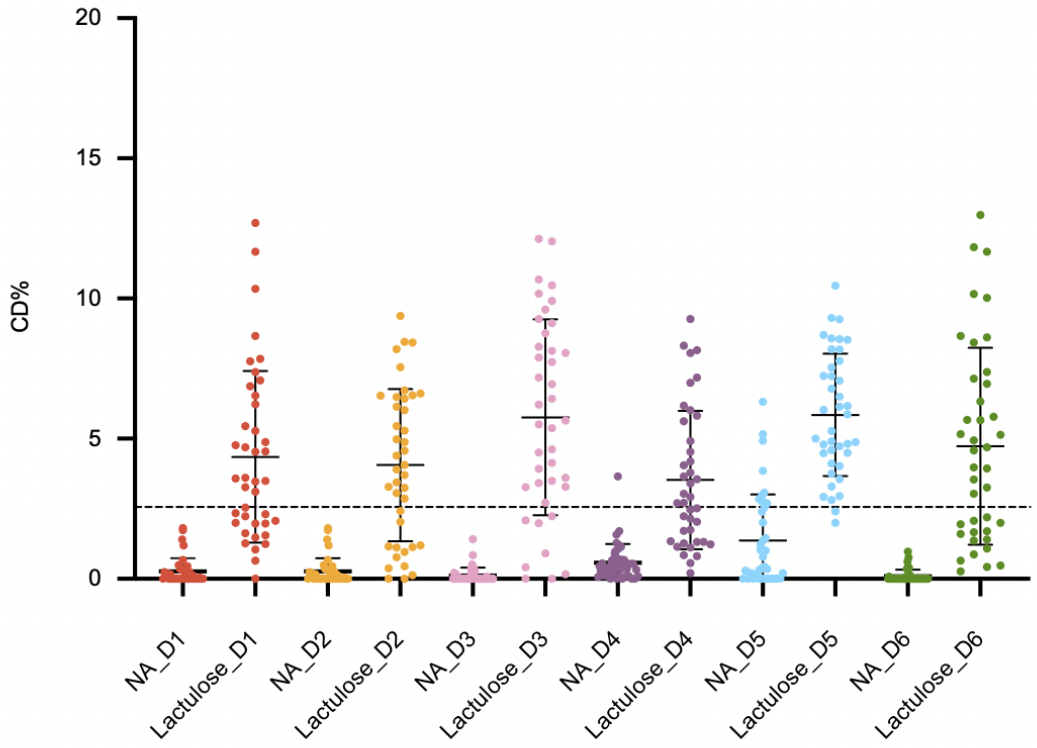

Figure 4. Comparison of all CD percentages of single cell measurements for donor 1-5 (D1-5) of lactulose amended and no amended samples (NA). *The x-axis represents D1-5 samples divided into samples incubated in the presence of lactulose or NA. Y-axis describes CD%. Calculations were generated by the testing tool Scattr with the following settings: alignment none, baselining polynomial at 3, normalization total spectrum. Each coloured dot represents the CD% of a Raman measurement for a single cell. The dashed line marks the threshold, which was determined by calculating the mean + 3 sd of the measurements of sample 3 amended with glucose and no D_2O. Threshold: ~2,56.*

3.2 Identification of single bacterial cells by RACS in the presence of XOS and lactulose

The detected incorporation of the D_2O levels with Raman spectroscopy allowed us to identify metabolic activity after XOS and lactulose supplementation. With RACS we aimed to identify the bacterial taxa able to utilize these compounds. Through targeted single cell isolation with Raman activated cell sorting we were able to isolate and identify specific bacteria strains in the presence of the prebiotic candidates XOS or lactulose. The percentage of deuterium labelled cells during the RACS process accounted between 0.84% and 21.62% (table 3) for samples amended with XOS and between 4.47% and 25.00% (table 4) for samples incubated with lactulose. After sorting we plated the sorted cells on YCFA-glucose to recover the isolated bacteria. To confirm the growth of the isolated microbes in the presence of the candidate prebiotic XOS or lactulose and therefore the ability to metabolise the compound we plated the single cells on YCFA-XOS or respectively YCFA-lactulose.

We were able to recover in total 49 single cells for samples incubated with the compound XOS from five of the six donors belonging to the two genera *Bifidobacterium* and *Collinsella* both from the phyla *Actinobacteria.* Seven different strains in total from these genera were isolated and identified with 16S rRNA gene sequencing: *Bifidobacterium adolescentis, Bifidobacterium faecale, Bifidobacterium longum, Bifidobacterium longum subsp. suillum, Bifidobacterium sp. and Collinsella aerofaciens* (table 5). Donor 1 was the one with the most diverse subset of isolated strains as 5 of the 6 isolated strains were present in the sample (table 5). The phylogenetic relationship of isolated strains is shown in figure 5. For donor 3 we were not able to isolate and identify a microbe of the gut community. There was a certain inter-individual variability between the donors regarding the single cells isolated for each donor as a consequence of the fundamental difference in their microbiome diversity as well as the integration of deuterium during metabolic processes.

All of these seven strains were able to grow in the presence of XOS by using YCFA media plates supplemented with XOS. Therefore, we suggest that *Bifidobacterium spp.* and *Collinsella aerofaciens* are probably primary XOS degraders.

Table 3. D-labelled and unlabelled cells of Raman activated cell sorting of samples amended with XOS. *Percentage of labelled cells and number of recovered cells including the percentage of recovery is shown. Deuterium (D)*

	Donors					
	D1	D2	D3	D4	D5	D6
D-labelled	26.00	8.00	4.00	8.00	14.00	1.00
Unlabelled	360.00	29.00	154.00	91.00	102.00	118.00
Total	386.00	37.00	158.00	99.00	116.00	119.00
Labelled (%)	6.74	21.62	2.53	8.08	12.07	0.84
Colonies recovered (n)	25.00	8.00	1.00	8.00	11.00	1.00
Recovery (%)	96.15	100.00	25.00	100.00	78.57	100.00

Table 4. D-labelled and unlabelled cells of Raman activated cell sorting of samples amended with lactulose*. Percentage of labelled cells and number of recovered cells including the percentage of recovery is shown. Deuterium (D).*

	Donors					
	D1	D2	D3	D4	D5	D6
D-labelled	24.00	10.00	7.00	21.00	21.00	7.00
Unlabelled	513.00	39.00	21.00	121.00	445.00	115.00
Total	537.00	49.00	28.00	142.00	466.00	122.00
Labelled (%)	4.47	20.41	25.00	14.79	4.51	5.74
Colonies recovered (n)	20.00	2.00	2.00	10.00	14.00	3.00
Recovery (%)	83.33	20.00	28.57	47.62	66.67	42.86

Table 5. Identified bacterial cells of samples amended with XOS in relation to the donor.

Identification of strains by colony PCR and 16S rRNA sanger sequencing, after RACS. Description of growth after RACS on rich media YCFA agar plates amended with XOS or glucose for all strains. Discrimination of positive growth (+) and no growth (-).

Strain	Growth on YCFA-XOS	Growth on YCFA-glucose	Present in donor
Bifidobacterium adolescentis	+	+	D1, D2, D5
Bifidobacterium faecale	+	+	D1, D2, D4, D5
Bifidobacterium longum	+	+	D4
Bifidobacterium longum subsp. suillum	+	+	D1, D2, D4, D6
Bifidobacterium sp.	+	+	D1, D2
Collinsella aerofaciens	+	+	D1, D4

For samples amended with the compound lactulose we were able to recover 48 single cells from five of the six donors belonging to the genera *Adlercreutzia, Bacteroides, Bifidobacterium, Collinsella, Enorma, Escherichia, Lactococcus and* unclassified *Lachnospiraceae* from the four phyla *Actinobacteria, Bacteroidetes, Firmicutes* and *Proteobacteria.* 17 different strains in total from these genera were isolated and identified with 16S rRNA gene sequencing*: Adlercreutzia hattorii, Adlercreutzia sp., Bacteroides sp., Bacteroides thetaiotaomicron, Bacteroides uniformis, Bifidobacterium adolescentis, Bifidobacterium faecale, Bifidobacterium longum, Bifidobacterium longum subsp. suillu, Bifidobacterium sp., Collinsella aerofaciens, Colinsella massiliensis, Collinsella sp., Escherichia coli, Lactococcus lactis and Lactococcus lactis subsp. hordniae (table 6).* The phylogenetic relationship of lactulose degraders is shown in figure 6.

For lactulose amended samples, not all of the identified strains were able to re-grow on YCFA-lactulose media plates, displayed also in table 6. This concerns the strains *Adlercreutzia hattorii, Adlercreutzia sp., Bacteroides sp., Bacteroides thetaiotaomicron, Bacteroides uniformis, Butyrate-producing bacterium,* some *Collinsella aerofaciens* isolates*, Colinsella massiliensis, Collinsella sp.* and *Escherichia coli.* This may be an indication for the strains being a secondary degrader rather than a primary degrader of lactulose. As primary degraders of lactulose we propose the isolates from the genera *Bifidobacterium, Lactococcus* and some specific strains of the genus *Collinsella.* These isolates were able to utilize lactulose and grow an YCFA media plates amended with lactulose. The variation between the different *Collinsella* strains may imply that only specified strains of this genera are able to utilize lactulose, noting that the differentiation of strains only with 16S rRNA gene sequencing is not sufficient.

Table 6 Identified bacterial cells of samples amended with lactulose in relation to the donor. *Identification of strains by colony PCR and 16S rRNA sanger sequencing, after RACS. Description of growth after RACS on rich media YCFA agar plates amended with lactulose or glucose for all strains. Discrimination of positive growth (+), no growth (-) and dissimilar (+/-) for isolates of the same strain.*

Strain	Growth on YCFA-lactulose	Growth on YCFA-glucose	Present in donor
Adlercreutzia hattorii	-	+	D4
Adlercreutzia sp.	-	+	D4
Bacteroides sp.	-	+	D1
Bacteroides thetaiotaomicron	-	+	D1
Bacteroides uniformis	-	+	D1, D4, D6
Bifidobacterium adolescentis	+	+	D1
Bifidobacterium faecale	+	+	D1, D4, D6
Bifidobacterium longum	+	+	D1
Bifidobacterium longum subsp. suillum	+	+	D4
Bifidobacterium sp.	+	+	D1, D4
Collinsella aerofaciens	+/-	+	D1, D5, D6
Collinsella massiliensis	-	+	D2
Collinsella sp.	-	+	D4
Escherichia coli	-	+	D1
Lactococcus lactis	+	+	D5
Lactococcus lactis subsp. hordniae	+	+	D5

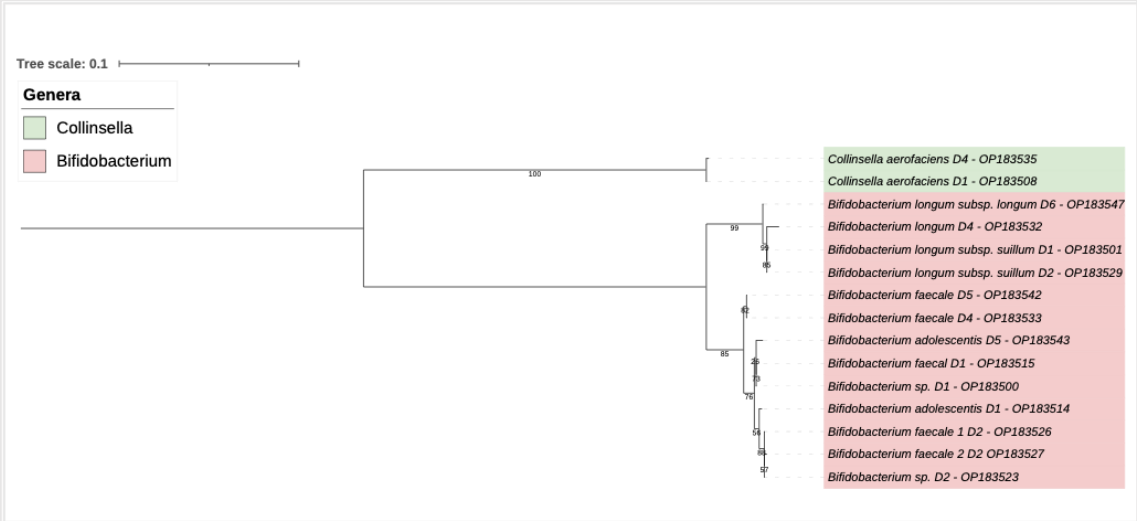

Figure 5. Phylogenetic relationship of isolated XOS degraders by RACS. *Individual strains were selected based on the 16S rRNA data as representation for other isolates of the same strain. The tree was generated with the maximum likelihood algorithm inclusive bootstrapping using IQtree. The model finder identified TN+F+G4 as the best-fit model for isolates of samples amended with XOS. The phylogenetic tree is midpoint rooted. Colours discriminate different genera (green: Collinsella and red: Bifidobacterium). Description of strains includes GenBank accession numbers (OP numbers).*

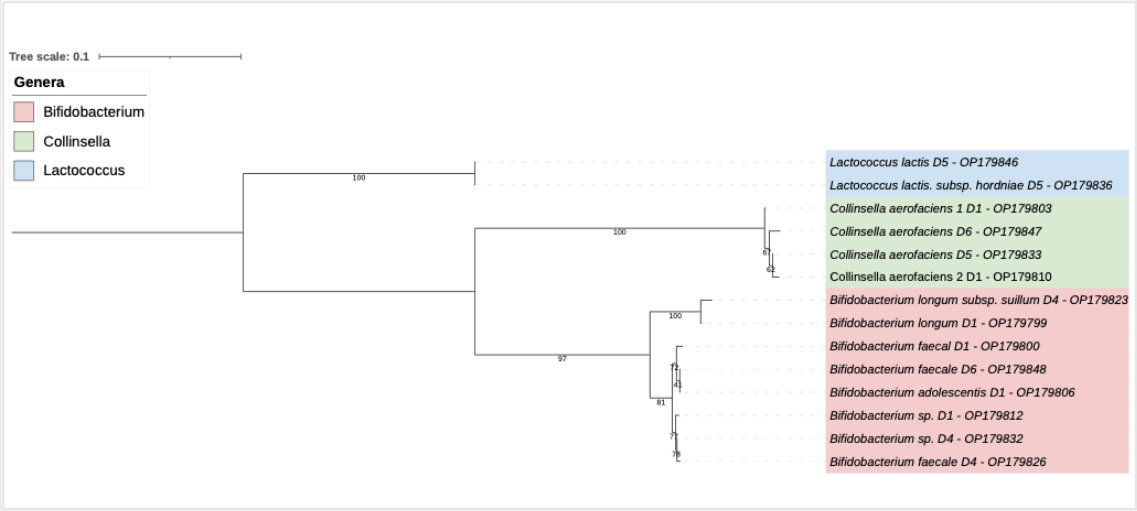

Figure 6. Phylogenetic relationship of lactulose degraders isolated by RACS. *Individual strains were selected based on the 16S rRNA data as representation for other isolates of the same strain. The tree was generated with the maximum likelihood algorithm inclusive bootstrapping using IQtree. The model finder identified K2P+G4 as the best-fit model for isolates of samples amended with lactulose. The phylogenetic tree is midpoint rooted. Colours discriminate different genera (blue: Lactococcus, green: Collinsella and red: Bifidobacterium). Description of strains includes GenBank accession numbers (OP numbers).*

4 Discussion

A range of prebiotics is known to selectively promote the growth of different gut bacteria, though mechanisms on individual bacteria level are often not fully evaluated. In our study, we elucidated the prebiotic effect of the compounds XOS and lactulose on the human gut microbiome by combining Raman microspectroscopy and Raman activated cell sorting with cultivation. We aimed to identify specific gut bacteria strains from human stool samples from 6 different donors to observe their responsiveness to the prebiotic candidate compounds XOS and lactulose. Raman microspectroscopy together with stable isotope-labelling with deuterium enables the identification of metabolic active cells in the presence of selected compounds, as the deuterium is incorporated into cells during the synthesis of mostly lipids, but also of nucleic acids, proteins and carbohydrates. Our analysis revealed higher metabolic activity in the presence of XOS or lactulose in comparison to no amended controls for all donor samples (figures 3 and 4). To further understand the metabolic processes on an individual level, we performed targeted single cell isolation using RACS. The total percentage of labelled bacterial cells and the recovery rates of RACS isolates differed between donors, described in detail in table 3 and 4. This may be explained by the presence of a donor-dependent gut microbiome and a diverse D_2O incorporation during metabolic processes.

For samples amended with XOS, we could recover 49 single cells from 5 of the 6 donors belonging to the gut community. We identified seven different strains from the genera *Bifidobacterium* and *Collinsella*: *Bifidobacterium adolescentis, Bifidobacterium faecale, Bifidobacterium longum, Bifidobacterium longum subsp. suillum, Bifidobacterium sp.* and *Collinsella aerofaciens.* Our findings support previous studies which identified *Bifidobacterium* taxa as XOS degraders[142–148].

Regarding samples amended with lactulose we were able to recover 48 single bacterial cells from 5 of the 6 donors from the genera *Adlercreutzia, Bacteroides, Bifidobacterium, Collinsella, Enorma, Escherichia, Lactococcus* and unclassified *Lachnospiraceae.* In total, we identified 17 different strains although not every isolate was able to utilize lactulose in the media for their growth. Therefore, we suggest taxa from the genera *Bifidobacterium, Lactococcus* and specific strains of *Collinsella* as primary degraders of lactulose. Regardless of the short incubation time other strains most likely incorporate deuterium as consequence of cross-feeding, as the primary degrades break down lactulose and release metabolites, which can be utilized by other commensals. For this reason, we hypothesize that the strains *Adlercreutzia hattorii, Adlercreutzia sp., Bacteroides sp., Bacteroides thetaiotaomicron, Bacteroides uniformis,* some *Collinsella aerofaciens isolates, Colinsella massiliensis, Collinsella sp.* and *Escherichia coli,* are probably secondary degraders, as they did not show any growth after isolation on YCFA-lactulose agar plates.

Bifidobacterium is a widely studied genus and is associated with health benefits, hence it can often be found in functional foods. Following species have been identified from stool smaples of healthy subjects, *B. adolescentis, B. animalis, B. bifidum, B. breve, B. catenulatum, B. dentium* and *B. pseudocatenulatu. B. animalis* and *B dentium*, are not considered autochthonous to the GIT as they are detected in faeces but not in mucosa-associated samples[149–151]. Numerous studies reported the bifidogenic effect of prebiotic compounds such as inulin, arabinoxylans, GOS and FOS correlating it to greater *Lactobacillus-Bifidobacterium* to *Enterobacteriaceae* ratio and change of SCFA production[149,152–154]. *Bifidobacterium* species contribute to the SCFA acid pool by metabolizing non-digestible dietary fibres and are known to preferentially utilize di-and oligosaccharides. Whole genome analysis revealed their genetic repertoire for the breakdown of complex carbohydrates. Yang et. al recently published data on the transcriptome activity of *Bifidobacterium adolescentis* 15703 in the presence of XOS, showing the upregulation of ABC transporters, β-xylosidase, β-galactosidase, β-glucosidase and α-amylases[155]. In addition, studies indicate their capability for the utilization of lactulose, matching our findings[40,156]. For example, Cui et. al showed by 16S rRNA gene amplicon sequencing of mice faeces, that lactulose significantly increased the relative abundance of *Bifidobacterium*[157].

Moreover, *Bifidobacterium* species contribute to hosts health by synthesizing some B vitamins including thiamine (B1), pyridoxine (B6), folic acid (B11) and nicotinic acid (B3)[158]. *In vitro* studies also demonstrated their ability to produce antimicrobial compounds like organic acids, iron-scavenging compounds and bacteriocins. Therefore, it is believed that *Bifidobacterium* species are involved in innate immune response of the host via interaction with Toll-like-receptors (TLRs)[159].

Conflicted data is available on the genus *Collinsella*, some studies indicate their role as pathobionts for example in irritable bowel syndrome[160] and psoriatic arthritis[161]. In other studies, *Collinsella spp.* is reported to be beneficial, as they ferment various carbohydrates including complex sugars for the production of hydrogen gas, ethanol, formate, lactate and the SCFA butyrate. *Collinsella* spp. can further deconjugate bile acids and are positively correlated with plasma cholesterol levels[162]. Our data suggest their ability to utilize complex polymers as XOS.

The genus *Lactococcus* can be subdivided into the subspecies *L. lactis subsp. lactis, L. lactis subsp. cremoris,* and *L. lactis subsp. hordniae*[163]. *L. lactis* has previously been shown to be able to grow on lactulose[164]. *Lactococcus spp.* often are utilized in fermentation processes during the production of cheese, yoghurt, sauerkraut and other pickled vegetables. Moreover, it is a commonly used probiotic strain, based on its anti-inflammatory properties. Apart from that, *Lactococcus* lactis functions as model lactic acid bacteria in genetic engineering, being used as cloning and expression system[163]. In the biomedical area it is used as in vivo delivery vector for various antigens and modulatory proteins[165].

In summary, our study demonstrated that cell sorting combined with cultivation is a powerful method to identify key gut microbes with the capability to degrade specific prebiotic compounds. XOS is a prebiotic compound with great potential for human health as human and animal studies demonstrated that low doses (1.4 g per day) are already efficacious to increase *Bifidobacterium* counts. In comparison, FOS and GOS are needed in higher amounts ≥ 10 g per day to be effective[166]. Moreover, XOS can be easily produced from xylan from abundant agriculture residues/by-products like corncobs, natural grass, pigeon pea stalks, green coconut husks and sugarcane bagasse[167].

Our findings support the bifidogenic effect of XOS but also [168] state that other genera like *Collinsella* are involved in the breakdown of the compound. We displayed that lactulose, despite the fact of its synthetic origin, promotes the growth of beneficial bacteria from the genera *Bifidobacterium, Lactococcus* and *Collinsella.* Also, our results indicate a broader effect of the substrate lactulose on the gut community by supporting interactions of cross-feeding. Potential candidates involved in this cross-feeding are strains like *Adlercreutzia, Bacteroides* and *Collinsella.* It is important to state, that supplementary data is necessary to prospectively interpret cross-feeding actions. Whole genome analysis will disclose the genetic potential of isolated individual strains to express the necessary enzymes β-xylosidases/α-galactosidase for XOS degradation and β-galactosidase for the metabolization of lactulose. Additionally, analysis of metabolic activity using High Performance Anion Exchange Chromatography (HPAEC) can be performed, to demonstrate utilization of the prebiotic compounds by specific isolates.

Our study helps understanding metabolic process in the gut microbiome, especially the characterization and involvement of individual strains. Moreover, it provides an original method for analysing the role of prebiotic compounds in the gut microbiome. This provides a basis for the safe application of pre- or synbiotics in the future. Additional co-culture experiments and the investigation of SCFAs can yield supplementary information to fully elucidate mechanisms of cross-feeding. Also, the declaration prebiotics includes a health benefit for the host, hence more clinical studies in humans should be conducted to complement the comprehension of the beneficial effect of XOS and lactulose on host's health.

Supplementary Tables and Figures

Supplementary Table 1. List of used software.

Software	
BLAST – basic local alignment search tool	NCBI https://blast.ncbi.nlm.nih.gov/Blast.cgi
DECIPHER	http://www2.decipher.codes/FindChimeras.html
iTOL	https://itol.embl.de
iQtree	http://www.iqtree.org
LabSpec 6	Horiba Scientific, France https://www.horiba.com/en_en/products/detail/action/show/Product/labspec-6-spectroscopy-suite-software-1843/
MATLAB 4.2	Mathworks, MA, USA https://de.mathworks.com/products/matlab.html
Nemesys	Cetoni, Korbussen, Germany https://www.cetoni.com/products/nemesys-userinterface/
NanoDrop ND - 1000	Peqlab Biotechnology, Germany
4Peaks 1.8	Nucleobytes, Amsterdam, Netherlands https://nucleobytes.com/4peaks/
Prism	Graphpad, San Diego, USA https://www.graphpad.com/scientific-software/prism/
Scattr – single cell analysis and testing tool for Raman microspectroscopy	http://shiny.csb.univie.ac.at:3838/scattr/
Serial Cloner 2.6	SerialBasic, http://serialbasics.free.fr/Serial_Cloner.html
Silva	Max Planck Institute for Marine Microbiology and Jacobs University, Bremen, Germany https://www.arb-silva.de/aligner/

Supplementary Table 2. Equipment list.

Equipment	Company
Anaerobic Chamber	Coy Laboratory Products, MI, USA
Anarobic Jar	Thermo Fisher Scientific, MA, USA
AnaeroGen™ 2.5L	Thermo Fisher Scientific, MA, USA
Aluminium coated slide A1136	EMF Corporatio, USA
Cannula (0,6 x 23 mm)	Transcodent, Germany
Centrifuge MiniSpin	Eppendorf, Germany
Centrifuge 5804 R	Eppendorf, Germany
Eppendort Research Plus Pipettes 1 - 1000	Eppendorf, Germany
Hamilton syringe 500 µl and 1 ml	Hamilton, NV, USA
High precision glass cover slip	Paul Marienfeld, Germany
InnuPREP PCRpure Kit	Analytik Jena, Germany
Laboratory Corona treater	Electro-Technic Products, IL, USA
NanoDrop ND-1000	Peqlab Biotechnology, Germany
Polyethylene tubing (0.97 mm OD x 0.58 mm ID)	Warner Instruments, CT, USA
Puncher (ø 0.75 mm)	WellTech, Taiwan
Raman microspectrometer LabRAM HR Evolution	Horiba Scientific, Japan
Raman microspectrometer LabRAM HR800	Horiba Scientific, Japan
Syringe System neMESYS 290N	Cetoni, Germany
Syringe Omnifix-FLuerSolo 1ml	Braun, Germany
T100 PCR thermal cycler	Bio-Rad Laboratories, CA, USA
Eppendorf tubes 1,5 ml	Eppendorf, Germany
UV Sterilisation PCR Workstation	PEQLAB Biotechnologie, Germany
Vortex-Genie 2	Scientific Industries, NY, USA
100X, 60X and 5X Microscope Objectives	Olympus, Japan

Supplementary Table 3. Chemical list.

Chemicals	Company
Agar	Sigma-Aldrich, USA
BSA 20mg/ml	Thermo Fisher Scientific, Germany
Base elastomer Sylgard 184™	Dow corning, MI, USA
Current agent Sylgard 184™	Dow corning, MI, USA
dNTPs 2mM	Thermo Fisher Scientific, Germany
Dream Taq Polymerase 5U/ $\boldsymbol{\mu l}$	Thermo Fisher Scientific, Germany
D_2O	Sigma-Aldrich, MO, USA
Fructose	Carl Roth, Germany
Galactose	Carl Roth, Germany
Glucose	Carl Roth, Germany
10x Green DreamTaq buffer including 20 $\boldsymbol{\mu m}$ $MgCl_2$	Thermo Fisher Scientific, Germany
H_2O PCR grade	Thermo Fisher Scientific, Germany
Lactulose	Carl Roth, Germany
MilliQ H_2O	Milipore, MA, USA
Primer forward 616V, 50 $\boldsymbol{\mu M}$	Thermo Fisher Scientific, Germany
Primer reversed 1492R, 50 $\boldsymbol{\mu M}$	Thermo Fisher Scientific, Germany
Xylose	Carl Roth, Germany
Xylooligosaccharides	Carl Roth, Germany

Supplementary Table 4. 10X Phosphate-buffered saline (PBS) stock solution.

10X Phosphate-buffered saline (PBS) stock solution (pH 7.2 – 7.4)	
Chemical	Concentration (g/l)
$Na_2HPO_4 \cdot 7H_2O$	25.6
NaCl	80
KCl	2
KH_2PO_4	2
Bring to 1 litre with H_2O and autoclave for 40 minutes at 121°C	

Supplementary Table 5. Production of rich medium yeast casitone fatty acids broth for agar plates.

YCFA medium (pH 6.8 – 6.9)	
Chemical	Concentration (g/l)
Casitone	10
Yeast extract	2.5
Glucose or lactulose or XOS	5
$MgSO_4$ x 7 H_2O	0.045
$CaCl_2$ x 2 H_2O	0.090
K_2HPO_4	0.45
KH_2PO_4	0.45
NaCl	0.9
Resazurin	0.001
Distilled water	1000 ml
$NaHCO_3$	4
L-Cysteine-HCl	1
Hemin	0.010
Volatile fatty acids	Concentration (ml/l)
Acetic acid	1.90
Propionic acid	0.70
iso-Butyric acid	0.09
n-Valeric acid	0.1
iso-Valeric acid	0.1
Vitamin solution *	Concentration (mg/l)
Biotin	2
Folic acid	2
Pyridoxine-HCl	10
Thiamine-HCl x 2 H_2O	5
Riboflavin	5
Nicotinic acid	5
D-Ca-pantothenate	5
Vitamin B_{12}	0.1
p-Aminobenzoic acid	5
Lipoic acid	5
Distilled water	1000 ml
Agar (15g/l) added for solid medium (plates) *Vitamin solution added after autoclaving	

Donor	Sequence ID	Genbank accession number	Media of isolation	Phylum	Class	Order	Family	Genus	Species	Best match (BLAST)
D1	RACS_DI73	OP183499	YCFA+XOS	Actinobacteria	Actinomycetia	Bifidobacteriales	Bifidobacteriaceae	Bifidobacterium	Bifidobacterium sp.	99,34
D1	RACS_DI74	OP183500	YCFA+XOS	Actinobacteria	Actinomycetia	Bifidobacteriales	Bifidobacteriaceae	Bifidobacterium	Bifidobacterium sp.	99,34
D1	RACS_DI75	OP183501	YCFA+XOS	Actinobacteria	Actinomycetia	Bifidobacteriales	Bifidobacteriaceae	Bifidobacterium	Bifidobacterium longum subsp. suillum	100
D1	RACS_DI76	OP183502	YCFA+XOS	Actinobacteria	Actinomycetia	Bifidobacteriales	Bifidobacteriaceae	Bifidobacterium	Bifidobacterium sp.	99,27
D1	RACS_DI77	OP183503	YCFA+XOS	Actinobacteria	Actinomycetia	Bifidobacteriales	Bifidobacteriaceae	Bifidobacterium	Bifidobacterium longum subsp. suillum	100
D1	RACS_DI78	OP183504	YCFA+XOS	Actinobacteria	Actinomycetia	Bifidobacteriales	Bifidobacteriaceae	Bifidobacterium	Bifidobacterium sp.	99,49
D1	RACS_DI79	OP183505	YCFA+XOS	Actinobacteria	Actinomycetia	Bifidobacteriales	Bifidobacteriaceae	Bifidobacterium	Collinella aerofaciens	99,89
D1	RACS_DI80	OP183506	YCFA+XOS	Actinobacteria	Actinomycetia	Bifidobacteriales	Bifidobacteriaceae	Bifidobacterium	Bifidobacterium longum subsp. suillum	100
D1	RACS_DI81	OP183507	YCFA+XOS	Actinobacteria	Actinomycetia	Bifidobacteriales	Bifidobacteriaceae	Bifidobacterium	Bifidobacterium longum subsp. suillum	100
D1	RACS_DI82	OP183508	YCFA+XOS	Actinobacteria	Coriobacteriia	Coriobacteriales	Coriobacteriaceae	Collinsella	Collinsella aerofaciens	99,89
D1	RACS_DI83	OP183509	YCFA+XOS	Actinobacteria	Actinomycetia	Bifidobacteriales	Bifidobacteriaceae	Bifidobacterium	Bifidobacterium sp.	99,27
D1	RACS_DI84	OP183510	YCFA+XOS	Actinobacteria	Actinomycetia	Bifidobacteriales	Bifidobacteriaceae	Bifidobacterium	Bifidobacterium sp.	99,27
D1	RACS_DI85	OP183511	YCFA+XOS	Actinobacteria	Actinomycetia	Bifidobacteriales	Bifidobacteriaceae	Bifidobacterium	Bifidobacterium faecale	99,21
D1	RACS_DI86	OP183512	YCFA+XOS	Actinobacteria	Actinomycetia	Bifidobacteriales	Bifidobacteriaceae	Bifidobacterium	Bifidobacterium faecale	99,27
D1	RACS_DI87	OP183513	YCFA+XOS	Actinobacteria	Actinomycetia	Bifidobacteriales	Bifidobacteriaceae	Bifidobacterium	Bifidobacterium longum subsp. suillum	100
D1	RACS_DI88	OP183514	YCFA+XOS	Actinobacteria	Actinomycetia	Bifidobacteriales	Bifidobacteriaceae	Bifidobacterium	Bifidobacterium adolescentis	99,57
D1	RACS_DI89	OP183515	YCFA+XOS	Actinobacteria	Actinomycetia	Bifidobacteriales	Bifidobacteriaceae	Bifidobacterium	Bifidobacterium faecale	99,19
D1	RACS_DI90	OP183516	YCFA+XOS	Actinobacteria	Actinomycetia	Bifidobacteriales	Bifidobacteriaceae	Bifidobacterium	Bifidobacterium sp.	99,26
D1	RACS_DI91	OP183517	YCFA+XOS	Actinobacteria	Actinomycetia	Bifidobacteriales	Bifidobacteriaceae	Bifidobacterium	Bifidobacterium longum subsp. suillum	100
D1	RACS_DI92	OP183518	YCFA+XOS	Actinobacteria	Actinomycetia	Bifidobacteriales	Bifidobacteriaceae	Bifidobacterium	Bifidobacterium longum subsp. suillum	100
D1	RACS_DI93	OP183519	YCFA+XOS	Actinobacteria	Actinomycetia	Bifidobacteriales	Bifidobacteriaceae	Bifidobacterium	Bifidobacterium faecal	99,34
D1	RACS_DI94	OP183520	YCFA+XOS	Actinobacteria	Coriobacteriia	Coriobacteriales	Coriobacteriaceae	Collinsella	Collinsella aerofaciens	99,76
D1	RACS_DI95	OP183521	YCFA+XOS	Actinobacteria	Actinomycetia	Bifidobacteriales	Bifidobacteriaceae	Bifidobacterium	Bifidobacterium longum subsp. suillum	100
D1	RACS_DI96	OP183522	YCFA+XOS	Actinobacteria	Actinomycetia	Bifidobacteriales	Bifidobacteriaceae	Bifidobacterium	Bifidobacterium longum subsp. suillum	100
D2	RACS_DI97	OP183523	YCFA+XOS	Actinobacteria	Actinomycetia	Bifidobacteriales	Bifidobacteriaceae	Bifidobacterium	Bifidobacterium sp.	99,34
D2	RACS_DI98	OP183524	YCFA+XOS	Actinobacteria	Actinomycetia	Bifidobacteriales	Bifidobacteriaceae	Bifidobacterium	Bifidobacterium longum subsp. suillum	100
D2	RACS_DI99	OP183525	YCFA+XOS	Actinobacteria	Actinomycetia	Bifidobacteriales	Bifidobacteriaceae	Bifidobacterium	Bifidobacterium adolescentis	100
D2	RACS_DI100	OP183526	YCFA+XOS	Actinobacteria	Actinomycetia	Bifidobacteriales	Bifidobacteriaceae	Bifidobacterium	Bifidobacterium faecale	99,35
D2	RACS_DI101	OP183527	YCFA+XOS	Actinobacteria	Actinomycetia	Bifidobacteriales	Bifidobacteriaceae	Bifidobacterium	Bifidobacterium faecale	99,42
D2	RACS_DI102	OP183528	YCFA+XOS	Actinobacteria	Actinomycetia	Bifidobacteriales	Bifidobacteriaceae	Bifidobacterium	Bifidobacterium adolescentis	99,45
D2	RACS_DI103	OP183529	YCFA+XOS	Actinobacteria	Actinomycetia	Bifidobacteriales	Bifidobacteriaceae	Bifidobacterium	Bifidobacterium longum subsp. suillum	100
D2	RACS_DI104	OP183530	YCFA+XOS	Actinobacteria	Actinomycetia	Bifidobacteriales	Bifidobacteriaceae	Bifidobacterium	Bifidobacterium longum subsp. suillum	100
D4	RACS_DI105	OP183531	YCFA+XOS	Actinobacteria	Actinomycetia	Bifidobacteriales	Bifidobacteriaceae	Bifidobacterium	Bifidobacterium longum	96,15
D4	RACS_DI106	OP183532	YCFA+XOS	Actinobacteria	Actinomycetia	Bifidobacteriales	Bifidobacteriaceae	Bifidobacterium	Bifidobacterium longum	96,68
D4	RACS_DI107	OP183533	YCFA+XOS	Actinobacteria	Actinomycetia	Bifidobacteriales	Bifidobacteriaceae	Bifidobacterium	Bifidobacterium faecale	99,71
D4	RACS_DI108	OP183534	YCFA+XOS	Actinobacteria	Coriobacteriia	Coriobacteriales	Coriobacteriaceae	Collinsella	Collinsella aerofaciens	98,78
D4	RACS_DI109	OP183535	YCFA+XOS	Actinobacteria	Coriobacteriia	Coriobacteriales	Coriobacteriaceae	Collinsella	Collinsella aerofaciens	99,85
D4	RACS_DI110	OP183536	YCFA+XOS	Actinobacteria	Actinomycetia	Bifidobacteriales	Bifidobacteriaceae	Bifidobacterium	Bifidobacterium longum subsp. suillum	99,91
D4	RACS_DI111	OP183537	YCFA+XOS	Actinobacteria	Actinomycetia	Bifidobacteriales	Bifidobacteriaceae	Bifidobacterium	Bifidobacterium faecale	99,71
D4	RACS_DI112	OP183538	YCFA+XOS	Actinobacteria	Actinomycetia	Bifidobacteriales	Bifidobacteriaceae	Bifidobacterium	Bifidobacterium faecale	99,64
D5	RACS_DI113	OP183539	YCFA+XOS	Actinobacteria	Actinomycetia	Bifidobacteriales	Bifidobacteriaceae	Bifidobacterium	Bifidobacterium faecale	99,78
D5	RACS_DI114	OP183540	YCFA+XOS	Actinobacteria	Actinomycetia	Bifidobacteriales	Bifidobacteriaceae	Bifidobacterium	Bifidobacterium faecale	99,40
D5	RACS_DI115	OP183541	YCFA+XOS	Actinobacteria	Actinomycetia	Bifidobacteriales	Bifidobacteriaceae	Bifidobacterium	Bifidobacterium faecale	99,71
D5	RACS_DI116	OP183542	YCFA+XOS	Actinobacteria	Actinomycetia	Bifidobacteriales	Bifidobacteriaceae	Bifidobacterium	Bifidobacterium faecale	99,78
D5	RACS_DI117	OP183543	YCFA+XOS	Actinobacteria	Actinomycetia	Bifidobacteriales	Bifidobacteriaceae	Bifidobacterium	Bifidobacterium adolescentis	96,52
D5	RACS_DI118	OP183544	YCFA+XOS	Actinobacteria	Actinomycetia	Bifidobacteriales	Bifidobacteriaceae	Bifidobacterium	Bifidobacterium faecale	100,00
D5	RACS_DI119	OP183545	YCFA+XOS	Actinobacteria	Actinomycetia	Bifidobacteriales	Bifidobacteriaceae	Bifidobacterium	Bifidobacterium faecale	99,78
D5	RACS_DI120	OP183546	YCFA+XOS	Actinobacteria	Actinomycetia	Bifidobacteriales	Bifidobacteriaceae	Bifidobacterium	Bifidobacterium faecale	98,91
D6	RACS_DI121	OP183547	YCFA+XOS	Actinobacteria	Actinomycetia	Bifidobacteriales	Bifidobacteriaceae	Bifidobacterium	Bifidobacterium longum subsp. longum	99,86

Supplementary Figure 1. All identified strains after RACS for samples amended with XOS. *Individual strains for donor 1-2 and 4-6 with GenBank accession number, media of isolation and best match in BLAST. Yellow marked strains were elected for phylogenetic tree generation.*

Donor	Sequence ID	GenBank accession number	Media of isolation	Phylum	Class	Order	Family	Genus	Species	Best match (BLAST)
D1	RACS_DI01	OP179799	YCFA+Lactulose	Actinobacteria	Actinomycetia	Bifidobacterilaes	Bifidobacteriaceae	Bifidobacterium	Bifidobacterium longum	100,00
D1	RACS_DI02	OP179800	YCFA+Lactulose	Actinobacteria	Actinomycetia	Bifidobacterilaes	Bifidobacteriaceae	Bifidobacterium	Bifidobacterium faecale	99,27
D1	RACS_DI03	OP179801	YCFA+Glucose	Actinobacteria	Coriobacteriia	Coriobacteriales	Coriobacteriaceae	Collinsella	Collinsella aerofaciens	99,86
D1	RACS_DI04	OP179802	YCFA+Glucose	Proteobacteria	Gammaproteobacteria	Enterobacterales	Enterobacteriaceae	Escherichia	Escherichia coli	99,57
D1	RACS_DI05	OP179803	YCFA+Lactulose	Actinobacteria	Coriobacteriia	Coriobacteriales	Coriobacteriaceae	Collinsella	Collinsella aerofaciens	97,51
D1	RACS_DI06	OP179804	YCFA+Glucose	Actinobacteria	Coriobacteriia	Coriobacteriales	Coriobacteriaceae	Collinsella	Collinsella aerofaciens	99,48
D1	RACS_DI07	OP179805	YCFA+Lactulose	Actinobacteria	Coriobacteriia	Coriobacteriales	Coriobacteriaceae	Collinsella	Collinsella aerofaciens	99,82
D1	RACS_DI08	OP179806	YCFA+Lactulose	Actinobacteria	Actinomycetia	Bifidobacterilaes	Bifidobacteriaceae	Bifidobacterium	Bifidobacterium adolescentis	100,00
D1	RACS_DI09	OP179807	YCFA+Glucose	Bacteroidetes	Bacteroidia	Bacteroidales	Bacteroidaceae	Bacteroides	Bacteroides sp.	99,93
D1	RACS_DI10	OP179808	YCFA+Lactulose	Actinobacteria	Coriobacteriia	Coriobacteriales	Coriobacteriaceae	Collinsella	Collinsella aerofaciens	99,82
D1	RACS_DI11	OP179809	YCFA+Glucose	Bacteroidetes	Bacteroidia	Bacteroidales	Bacteroidaceae	Bacteroides	Bacteroides thetaiotaomicron	98,46
D1	RACS_DI12	OP179810	YCFA+Lactulose	Actinobacteria	Coriobacteriia	Coriobacteriales	Coriobacteriaceae	Collinsella	Collinsella aerofaciens	99,73
D1	RACS_DI13	OP179811	YCFA+Glucose	Bacteroidetes	Bacteroidia	Bacteroidales	Bacteroidaceae	Bacteroides	Bacteroides uniformis	99,93
D1	RACS_DI14	OP179812	YCFA+Lactulose	Actinobacteria	Actinomycetia	Bifidobacterilaes	Bifidobacteriaceae	Bifidobacterium	Bifidobacterium sp.	99,35
D1	RACS_DI15	OP179813	YCFA+Lactulose	Actinobacteria	Coriobacteriia	Coriobacteriales	Coriobacteriaceae	Collinsella	Collinsella aerofaciens	99,65
D1	RACS_DI16	OP179814	YCFA+Glucose	Actinobacteria	Coriobacteriia	Coriobacteriales	Coriobacteriaceae	Collinsella	Collinsella aerofaciens	99,72
D1	RACS_DI17	OP179815	YCFA+Lactulose	Actinobacteria	Actinomycetia	Bifidobacterilaes	Bifidobacteriaceae	Bifidobacterium	Bifidobacterium sp.	99,63
D1	RACS_DI18	OP179816	YCFA+Glucose	Actinobacteria	Coriobacteriia	Coriobacteriales	Coriobacteriaceae	Collinsella	Collinsella aerofaciens	99,34
D1	RACS_DI19	OP179817	YCFA+Lactulose	Actinobacteria	Coriobacteriia	Coriobacteriales	Coriobacteriaceae	Collinsella	Collinsella aerofaciens	99,82
D1	RACS_DI20	OP179818	YCFA+Glucose	Bacteroidetes	Bacteroidia	Bacteroidales	Bacteroidaceae	Bacteroides	Bacteroides sp.	99,93
D2	RACS_DI21	OP179819	YCFA+Glucose	Actinobacteria	Coriobacteriia	Coriobacteriales	Coriobacteriaceae	Enorma	Colinsella massiliensis	99,12
D2	RACS_DI22	OP179820	YCFA+Glucose	Actinobacteria	Coriobacteriia	Coriobacteriales	Coriobacteriaceae	Enorma	Colinsella massiliensis	99,32
D4	RACS_DI25	OP179823	YCFA+Lactulose	Actinobacteria	Actinomycetia	Bifidobacterilaes	Bifidobacteriaceae	Bifidobacterium	Bifidobacterium longum subsp. suillum	96,32
D4	RACS_DI26	OP179824	YCFA+Lactulose	Actinobacteria	Actinomycetia	Bifidobacterilaes	Bifidobacteriaceae	Bifidobacterium	Bifidobacterium faecale	99,70
D4	RACS_DI28	OP179826	YCFA+Lactulose	Actinobacteria	Actinomycetia	Bifidobacterilaes	Bifidobacteriaceae	Bifidobacterium	Bifidobacterium faecale	99,70
D4	RACS_DI29	OP179827	YCFA+Glucose	Actinobacteria	Coriobacteriia	Coriobacteriales	Coriobacteriaceae	Collinsella	Collinsella sp.	100
D4	RACS_DI30	OP179828	YCFA+Glucose	Actinobacteria	Coriobacteriia	Eggerthellales	Eggerthellacea	Adlercreutzia	Adlercreutzia hattorii	99,63
D4	RACS_DI31	OP179829	YCFA+Glucose	Actinobacteria	Coriobacteriia	Eggerthellales	Eggerthellacea	Adlercreutzia	Adlercreutzia sp.	99,63
D4	RACS_DI32	OP179830	YCFA+Glucose	Bacteroidetes	Bacteroidia	Bacteroidales	Bacteroidaceae	Bacteroides	Bacteroides uniformis	99,78
D4	RACS_DI33	OP179831	YCFA+Glucose	Actinobacteria	Coriobacteriia	Eggerthellales	Eggerthellacea	Adlercreutzia	Adlercreutzia sp.	99,7
D4	RACS_DI34	OP179832	YCFA+Lactulose	Actinobacteria	Actinomycetia	Bifidobacterilaes	Bifidobacteriaceae	Bifidobacterium	Bifidobacterium sp.	99,87
D5	RACS_DI35	OP179833	YCFA+Lactulose	Actinobacteria	Coriobacteriia	Coriobacteriales	Coriobacteriaceae	Collinsella	Collinsella aerofaciens	98,25
D5	RACS_DI36	OP179834	YCFA+Lactulose	Actinobacteria	Coriobacteriia	Coriobacteriales	Coriobacteriaceae	Collinsella	Collinsella aerofaciens	100,00
D5	RACS_DI37	OP179835	YCFA+Lactulose	Actinobacteria	Coriobacteriia	Coriobacteriales	Coriobacteriaceae	Collinsella	Collinsella aerofaciens	96,99
D5	RACS_DI38	OP179836	YCFA+Lactulose	Firmicutes	Bacilli	Lactobacillales	Streptococcaceae	Lactococcus	Lactococcus lactis subsp. hordniae	100,00
D5	RACS_DI39	OP179837	YCFA+Lactulose	Actinobacteria	Coriobacteriia	Coriobacteriales	Coriobacteriaceae	Collinsella	Collinsella aerofaciens	98,53
D5	RACS_DI40	OP179838	YCFA+Lactulose	Actinobacteria	Coriobacteriia	Coriobacteriales	Coriobacteriaceae	Collinsella	Collinsella aerofaciens	98,14
D5	RACS_DI41	OP179839	YCFA+Lactulose	Actinobacteria	Coriobacteriia	Coriobacteriales	Coriobacteriaceae	Collinsella	Collinsella aerofaciens	96,62
D5	RACS_DI42	OP179840	YCFA+Lactulose	Actinobacteria	Coriobacteriia	Coriobacteriales	Coriobacteriaceae	Collinsella	Collinsella aerofaciens	97,54
D5	RACS_DI43	OP179841	YCFA+Lactulose	Actinobacteria	Coriobacteriia	Coriobacteriales	Coriobacteriaceae	Collinsella	Collinsella aerofaciens	98,42
D5	RACS_DI44	OP179842	YCFA+Lactulose	Actinobacteria	Coriobacteriia	Coriobacteriales	Coriobacteriaceae	Collinsella	Collinsella aerofaciens	96,04
D5	RACS_DI45	OP179843	YCFA+Lactulose	Firmicutes	Bacilli	Lactobacillales	Streptococcaceae	Lactococcus	Lactococcus lactis	100,00
D5	RACS_DI46	OP179844	YCFA+Lactulose	Actinobacteria	Coriobacteriia	Coriobacteriales	Coriobacteriaceae	Collinsella	Collinsella aerofaciens	97,20
D5	RACS_DI47	OP179845	YCFA+Lactulose	Actinobacteria	Coriobacteriia	Coriobacteriales	Coriobacteriaceae	Collinsella	Collinsella aerofaciens	98,94
D5	RACS_DI48	OP179846	YCFA+Lactulose	Firmicutes	Bacilli	Lactobacillales	Streptococcaceae	Lactococcus	Lactococcus lactis	100,00
D6	RACS_DI49	OP179847	YCFA+Lactulose	Actinobacteria	Coriobacteriia	Coriobacteriales	Coriobacteriaceae	Collinsella	Collinsella aerofaciens	97,65
D6	RACS_DI50	OP179848	YCFA+Lactulose	Actinobacteria	Actinomycetia	Bifidobacterilaes	Bifidobacteriaceae	Bifidobacterium	Bifidobacterium faecale	97,09
D6	RACS_DI51	OP179849	YCFA+Glucose	Bacteroidetes	Bacteroidia	Bacteroidales	Bacteroidaceae	Bacteroides	Bacteroides uniformis	99,93

Supplementary Figure 2. All identified strains after RACS for samples amended with lactulose*. Individual strains for donor 1-2 and 4-6 with GenBank accession number, media of isolation and best match in BLAST. Yellow marked strains were elected for phylogenetic tree generation.*

German Abstract

Es ist bekannt, dass ein breites Spektrum an präbiotischen Verbindungen das Darmmikrobiom stimulieren kann. Hier haben wir die Wirkung der präbiotischen Verbindungen Xylooligosaccharide (XOS) und Laktulose auf einzelne Bakterien des menschlichen Darmmikrobioms untersucht und gleichzeitig grundlegende Methoden für die Untersuchung präbiotischer Auswirkungen bereitgestellt. Zunächst analysierten wir die Stoffwechselaktivität in Anwesenheit von XOS und Laktulose in menschlichen Fäkalproben von sechs verschiedenen Probanden, indem wir Raman-Mikrospektroskopie zusammen mit Deuterium-Isotopenmarkierung angewandt haben. Deuterium wird während der zellulären Biosynthese von hauptsächlich Lipiden in die Zellen eingebaut und ermöglicht daher die Analyse metabolisch aktiver Zellen. Dabei zeigte sich für alle Proben eine höhere Stoffwechselaktivität in Anwesenheit von XOS oder Laktulose im Vergleich zu nicht supplementierten Proben. Um einzelne Taxa zu identifizieren, die durch XOS oder Laktulose stimuliert werden, führten wir eine Raman-aktivierte Zellsortierung und Kultivierung durch. Die 16rRNA-Sequenzierung der isolierten Bakterien ergab, dass Taxa aus den Gattungen *Bifidobacterium* und *Collinsella* in der Lage waren, sowohl die Verbindung XOS als auch Laktulose zu metabolisieren. Außerdem konnten wir Taxa aus der Gattung *Lactococcus* als Laktulose Verwerter identifizieren. Weiters deuten unsere Ergebnisse darauf hin, dass in Gegenwart von Laktulose Cross-feeding stattfindet. Potenzielle sekundäre Laktulose Verwerter könnten Mitglieder der Gattung *Adlercreutzia, Bacteroides* und bestimmte Taxa von *Collinsella* sein.

References

1. Rajili C-Stojanovi, M. & de Vos, W. M. The first 1000 cultured species of the human gastrointestinal microbiota. *FEMS Microbiologie Reviews* **38**, 996–1047 (2014).
2. Adak, A. & Khan, M. R. An insight into gut microbiota and its functionalities. *Cellular and Molecular Life Sciences* vol. 76 473–493 Preprint at (2019).
3. Tsai, Y.-L. *et al.* Probiotics, prebiotics and amelioration of diseases. *J Biomed Sci* **26**, 3 (2019).
4. Kundu, P., Blacher, E., Elinav, E. & Pettersson, S. Our Gut Microbiome: The Evolving Inner Self. *Cell* **171**, 1481–1493 (2017).
5. Perez-Muñoz, M. E., Arrieta, M. C., Ramer-Tait, A. E. & Walter, J. A critical assessment of the “sterile womb” and “in utero colonization” hypotheses: implications for research on the pioneer infant microbiome. *Microbiome* **5**, (2017).
6. Milani, C. *et al.* The First Microbial Colonizers of the Human Gut: Composition, Activities, and Health Implications of the Infant Gut Microbiota. *Microbiology and Molecular Biology Reviews* **81**, (2017).
7. Biasucci, G. *et al.* Mode of delivery affects the bacterial community in the newborn gut. *Early Hum Dev* **86**, 13–15 (2010).
8. Dominguez-Bello, M. G. *et al.* Delivery mode shapes the acquisition and structure of the initial microbiota across multiple body habitats in newborns. *Proc Natl Acad Sci U S A* **107**, 11971–11975 (2010).
9. le Hurou-Luron, I., Blat, S. & Boudry, G. Breast- v. formula-feeding: Impacts on the digestive tract and immediate and long-term health effects. *Nutr Res Rev* **23**, 23–36 (2010).
10. Koenig, J. E. *et al.* Succession of microbial consortia in the developing infant gut microbiome. *Proceedings of the National Academy of Sciences* **108**, 4578–4585 (2011).
11. Tanaka, M. & Nakayama, J. Development of the gut microbiota in infancy and its impact on health in later life. *Allergol Int* **66**, 515–522 (2017).
12. Bäckhed, F. *et al.* Dynamics and Stabilization of the Human Gut Microbiome during the First Year of Life. *Cell Host Microbe* **17**, 690–703 (2015).

13. Derrien, M., Alvarez, A.-S. & de Vos, W. M. The Gut Microbiota in the First Decade of Life. *Trends Microbiol* **27**, 997–1010 (2019).
14. Khanna, S. & Tosh, P. K. A clinician's primer on the role of the microbiome in human health and disease. *Mayo Clin Proc* **89**, 107–114 (2014).
15. Adak, A. & Khan, M. R. An insight into gut microbiota and its functionalities. *Cellular and Molecular Life Sciences* **76**, 473–493 (2019).
16. Aidy, S. E., van den Bogert, B. & Kleerebezem, M. The small intestine microbiota, nutritional modulation and relevance for health. *Curr Opin Biotechnol* **32**, 14–20 (2015).
17. Eckburg, P. B. *et al.* Diversity of the Human Intestinal Microbial Flora. *Science (1979)* **308**, 1635–1638 (2005).
18. Mariat, D. *et al.* The firmicutes/bacteroidetes ratio of the human microbiota changes with age. *BMC Microbiol* **9**, 1–6 (2009).
19. Barko, P. C., McMichael, M. A., Swanson, K. S. & Williams, D. A. The Gastrointestinal Microbiome: A Review. *J Vet Intern Med* **32**, 9–25 (2018).
20. Kaoutari, A. el, Armougom, F., Gordon, J. I., Raoult, D. & Henrissat, B. The abundance and variety of carbohydrate-active enzymes in the human gut microbiota. *Nature Reviews Microbiology 2013 11:7* **11**, 497–504 (2013).
21. Anderson, J. W. *et al.* Health benefits of dietary fiber. *Nutr Rev* **67**, 188–205 (2009).
22. Martens, E. C. *et al.* Recognition and degradation of plant cell wall polysaccharides by two human gut symbionts. *PLoS Biol* **9**, (2011).
23. Wardman, J. F., Bains, R. K., Rahfeld, P. & Withers, S. G. Carbohydrate-active enzymes (CAZymes) in the gut microbiome. *Nature Reviews Microbiology 2022 20:9* **20**, 542–556 (2022).
24. Drula, E. *et al.* The carbohydrate-active enzyme database: functions and literature. *Nucleic Acids Res* **50**, D571–D577 (2022).
25. McNeil, N. I. The contribution of the large intestine to energy supplies in man. *Am J Clin Nutr* **39**, 338–342 (1984).
26. Koh, A., de Vadder, F., Kovatcheva-Datchary, P. & Bäckhed, F. From Dietary Fiber to Host Physiology: Short-Chain Fatty Acids as Key Bacterial Metabolites. *Cell* **165**, 1332–1345 (2016).
27. Schnorr, S. L. *et al.* Gut microbiome of the Hadza hunter-gatherers. *Nat Commun* **5**, (2014).

28. Sonnenburg, E. D. *et al.* Diet-induced extinction in the gut microbiota compounds over generations. *Nature* **529**, 212 (2016).
29. Cummings, J. H., Pomare, E. W., Branch, H. W. J., Naylor, C. P. E. & MacFarlane, G. T. Short chain fatty acids in human large intestine, portal, hepatic and venous blood. *Gut* **28**, 1221–1227 (1987).
30. Kumar, J., Rani, K. & Datt, C. Molecular link between dietary fibre, gut microbiota and health. *Mol Biol Rep* **47**, 6229–6237 (2020).
31. Karaki, S. I. *et al.* Short-chain fatty acid receptor, GPR43, is expressed by enteroendocrine cells and mucosal mast cells in rat intestine. *Cell Tissue Res* **324**, 353–360 (2006).
32. Cummings, J. H. & Macfarlane, G. T. The control and consequences of bacterial fermentation in the human colon. *J Appl Bacteriol* **70**, 443–459 (1991).
33. Ragsdale, S. W. & Pierce, E. Acetogenesis and the Wood-Ljungdahl Pathway of CO2 Fixation. *Biochim Biophys Acta* **1784**, 1873 (2008).
34. Louis, P. *et al.* Restricted distribution of the butyrate kinase pathway among butyrate-producing bacteria from the human colon. *J Bacteriol* **186**, 2099–2106 (2004).
35. Duncan, S. H., Barcenilla, A., Stewart, C. S., Pryde, S. E. & Flint, H. J. Acetate Utilization and Butyryl Coenzyme A (CoA):Acetate-CoA Transferase in Butyrate-Producing Bacteria from the Human Large Intestine. *Appl Environ Microbiol* **68**, 5186 (2002).
36. Hetzel, M. *et al.* Acryloyl-CoA reductase from Clostridium propionicum. An enzyme complex of propionyl-CoA dehydrogenase and electron-transferring flavoprotein. *Eur J Biochem* **270**, 902–910 (2003).
37. Scott, K. P., Martin, J. C., Campbell, G., Mayer, C. D. & Flint, H. J. Whole-genome transcription profiling reveals genes up-regulated by growth on fucose in the human gut bacterium 'Roseburia inulinivorans'. *J Bacteriol* **188**, 4340–4349 (2006).
38. Wong, J. M. W., de Souza, R., Kendall, C. W. C., Emam, A. & Jenkins, D. J. A. Colonic Health: Fermentation and Short Chain Fatty Acids. *J Clin Gastroenterol* **40**, 235–243 (2006).
39. Louis, P. & Flint, H. J. Formation of propionate and butyrate by the human colonic microbiota. *Environ Microbiol* **19**, 29–41 (2017).

40. Karakan, T., Tuohy, K. M. & Janssen-van Solingen, G. Low-Dose Lactulose as a Prebiotic for Improved Gut Health and Enhanced Mineral Absorption. *Front Nutr* **8**, (2021).
41. Frost, G. *et al.* The short-chain fatty acid acetate reduces appetite via a central homeostatic mechanism. *Nat Commun* **5**, (2014).
42. Bergman, E. N. Energy contributions of volatile fatty acids from the gastrointestinal tract in various species. *Physiol Rev* **70**, 567–590 (1990).
43. Martin-Gallausiaux, C., Marinelli, L., Blottière, H. M., Larraufie, P. & Lapaque, N. Conference on diet and digestive disease symposium 2: Sensing and signalling of the gut environment: Scfa: Mechanisms and functional importance in the gut. *Proceedings of the Nutrition Society* **80**, 37–49 (2021).
44. Fleming, S. E., Choi, S. Y. & Fitch, M. D. Absorption of short-chain fatty acids from the rat cecum in vivo. *J Nutr* **121**, 1787–1797 (1991).
45. Ardawi, M. S. M. & Newsholme, E. A. Fuel utilization in colonocytes of the rat. *Biochem J* **231**, 713–719 (1985).
46. Roediger, W. E. W. Role of anaerobic bacteria in the metabolic welfare of the colonic mucosa in man. *Gut* **21**, 793–798 (1980).
47. Donohoe, D. R. *et al.* The Warburg effect dictates the mechanism of butyrate-mediated histone acetylation and cell proliferation. *Mol Cell* **48**, 612–626 (2012).
48. Lupton, J. R. Microbial degradation products influence colon cancer risk: the butyrate controversy. *J Nutr* **134**, 479–482 (2004).
49. Morrison, D. J. & Preston, T. Formation of short chain fatty acids by the gut microbiota and their impact on human metabolism. *Gut Microbes* **7**, 189–200 (2016).
50. Kelly, C. J. *et al.* Crosstalk between Microbiota-Derived Short-Chain Fatty Acids and Intestinal Epithelial HIF Augments Tissue Barrier Function. *Cell Host Microbe* **17**, 662–671 (2015).
51. Blaak, E. E. *et al.* Short chain fatty acids in human gut and metabolic health. *Benef Microbes* **11**, 411–455 (2020).
52. Pelaseyed, T. *et al.* The mucus and mucins of the goblet cells and enterocytes provide the first defense line of the gastrointestinal tract and interact with the immune system. *Immunol Rev* **260**, 8 (2014).

53. Burger-van Paassen, N. *et al.* The regulation of intestinal mucin MUC2 expression by short-chain fatty acids: implications for epithelial protection. *Biochem J* **420**, 211–219 (2009).
54. Hatayama, H., Iwashita, J., Kuwajima, A. & Abe, T. The short chain fatty acid, butyrate, stimulates MUC2 mucin production in the human colon cancer cell line, LS174T. *Biochem Biophys Res Commun* **356**, 599–603 (2007).
55. Cani, P. D. *et al.* Changes in gut microbiota control metabolic endotoxemia-induced inflammation in high-fat diet-induced obesity and diabetes in mice. *Diabetes* **57**, 1470–1481 (2008).
56. Tolhurst, G. *et al.* Short-Chain Fatty Acids Stimulate Glucagon-Like Peptide-1 Secretion via the G-Protein–Coupled Receptor FFAR2. *Diabetes* **61**, 364–371 (2012).
57. Chambers, E. S., Morrison, D. J. & Frost, G. Control of appetite and energy intake by SCFA: what are the potential underlying mechanisms? *Proc Nutr Soc* **74**, 328–336 (2015).
58. Larraufie, P. *et al.* SCFAs strongly stimulate PYY production in human enteroendocrine cells. *Scientific Reports 2017 8:1* **8**, 1–9 (2018).
59. Brooks, L. *et al.* Fermentable carbohydrate stimulates FFAR2-dependent colonic PYY cell expansion to increase satiety. *Mol Metab* **6**, 48–60 (2016).
60. Li, M. *et al.* Pro- and anti-inflammatory effects of short chain fatty acids on immune and endothelial cells. *Eur J Pharmacol* **831**, 52–59 (2018).
61. Huang, W., Zhou, L., Guo, H., Xu, Y. & Xu, Y. The role of short-chain fatty acids in kidney injury induced by gut-derived inflammatory response. *Metabolism* **68**, 20–30 (2017).
62. Akimova, T., Beier, U. H., Liu, Y., Wang, L. & Hancock, W. W. Histone/protein deacetylases and T-cell immune responses. *Blood* **119**, 2443–2451 (2012).
63. Schilderink, R., Verseijden, C. & de Jonge, W. J. Dietary Inhibitors of Histone Deacetylases in Intestinal Immunity and Homeostasis. *Front Immunol* **4**, (2013).
64. Yu, X. *et al.* Short-chain fatty acids from periodontal pathogens suppress histone deacetylases, EZH2, and SUV39H1 to promote Kaposi's sarcoma-associated herpesvirus replication. *J Virol* **88**, 4466–4479 (2014).
65. Reichardt, N. *et al.* Phylogenetic distribution of three pathways for propionate production within the human gut microbiota. *The ISME Journal 2014 8:6* **8**, 1323–1335 (2014).

66. Saa, P., Urrutia, A., Silva-Andrade, C., Martín, A. J. & Garrido, D. Modeling approaches for probing cross-feeding interactions in the human gut microbiome. *Comput Struct Biotechnol J* **20**, 79–89 (2022).
67. Cavaliere, M., Feng, S., Soyer, O. S. & Jiménez, J. I. Cooperation in microbial communities and their biotechnological applications. *Environ Microbiol* **19**, 2949–2963 (2017).
68. Holscher, H. D. Dietary fiber and prebiotics and the gastrointestinal microbiota. *Gut Microbes* **8**, 172–184 (2017).
69. Rivière, A., Selak, M., Lantin, D., Leroy, F. & de Vuyst, L. Bifidobacteria and butyrate-producing colon bacteria: Importance and strategies for their stimulation in the human gut. *Front Microbiol* **7**, (2016).
70. Gibson, G. R. & Roberfroid, M. B. Dietary modulation of the human colonic microbiota: introducing the concept of prebiotics. *J Nutr* **125**, 1401–1412 (1995).
71. Gibson, G. R. *et al.* Expert consensus document: The International Scientific Association for Probiotics and Prebiotics (ISAPP) consensus statement on the definition and scope of prebiotics. *Nat Rev Gastroenterol Hepatol* **14**, 491–502 (2017).
72. Brosseau, C. *et al.* Prebiotics: Mechanisms and Preventive Effects in Allergy. *Nutrients* **11**, 1841 (2019).
73. Lockyer, S. & Stanner, S. Prebiotics – an added benefit of some fibre types. *Nutr Bull* **44**, 74–91 (2019).
74. Flores-Maltos, D. A. *et al.* Biotechnological production and application of fructooligosaccharides. *Crit Rev Biotechnol* **36**, 259–267 (2016).
75. Wilson, B. & Whelan, K. Prebiotic inulin-type fructans and galacto-oligosaccharides: definition, specificity, function, and application in gastrointestinal disorders. *J Gastroenterol Hepatol* **32 Suppl 1**, 64–68 (2017).
76. Goulas, A., Tzortzis, G. & Gibson, G. R. Development of a process for the production and purification of α- and β-galactooligosaccharides from Bifidobacterium bifidum NCIMB 41171. *Int Dairy J* **17**, 648–656 (2007).
77. Loo, J. van, Clune, Y., Bennett, M. & Collins, J. K. The SYNCAN project: goals, set-up, first results and settings of the human intervention study. *British Journal of Nutrition* **93**, S91–S98 (2005).

78. Loo, J. van, Coussement, P., de Leenheer, L., Hoebreg, H. & Smits, G. On the presence of Inulin and Oligofructose as natural ingredients in the western diet. *Crit Rev Food Sci Nutr* **35**, 525–552 (2009).
79. Vázquez, M. J., Alonso, J. L., Domínguez, H. & Parajó, J. C. Xylooligosaccharides: Manufacture and applications. *Trends Food Sci Technol* **11**, 387–393 (2000).
80. Mhetras, N., Mapre, V. & Gokhale, D. Xylooligosaccharides (XOS) as Emerging Prebiotics: Its Production from Lignocellulosic Material. *Adv Microbiol* **9**, 14–20 (2019).
81. Akpinar, O., Ak, O., Kavas, A., Bakir, U. & Yilmaz, L. Enzymatic production of xylooligosaccharides from cotton stalks. *J Agric Food Chem* **55**, 5544–5551 (2007).
82. Zhang, B., Zhong, Y., Dong, D., Zheng, Z. & Hu, J. Gut microbial utilization of xylan and its implication in gut homeostasis and metabolic response. *Carbohydr Polym* **286**, 119271 (2022).
83. Rohman, A., Dijkstra, B. W. & Puspaningsih, N. N. T. β-Xylosidases: Structural Diversity, Catalytic Mechanism, and Inhibition by Monosaccharides. *Int J Mol Sci* **20**, (2019).
84. Domingues, R. *et al.* Xylose Metabolism in Bacteria—Opportunities and Challenges towards Efficient Lignocellulosic Biomass-Based Biorefineries. *Applied Sciences 2021, Vol. 11, Page 8112* **11**, 8112 (2021).
85. Pranami, D., Sharma, R. & Pathak, H. Lactulose: a prebiotic, laxative and detoxifying agent. *Drugs and Therapy Perspectives* **33**, 228–233 (2017).
86. Petuely, F. The Lactobacillus bifidus factor. *Dtsch Med Wochenschr* **82**, 1957–1960 (1957).
87. Schuster-Wolff-Bühring, R., Fischer, L. & Hinrichs, J. Production and physiological action of the disaccharide lactulose. *Int Dairy J* **20**, 731–741 (2010).
88. Mylan. Duphalac 3.335 g/5 ml Oral Solution Summary of Product Characteristics. Hatfield (2020). https://www.medicines.org.uk/emc/product/5525/smpc#gref.
89. Cecchini, D. A. *et al.* Functional Metagenomics Reveals Novel Pathways of Prebiotic Breakdown by Human Gut Bacteria. *PLoS One* **8**, 72766 (2013).

90. Sen, T. *et al.* Diet-driven microbiota dysbiosis is associated with vagal remodeling and obesity HHS Public Access Author manuscript. *Physiol Behav* **173**, 305–317 (2017).
91. Weiss, G. A. & Hennet, T. Mechanisms and consequences of intestinal dysbiosis. *Cellular and Molecular Life Sciences* **74**, 2959–2977 (2017).
92. le Chatelier, E. *et al.* Richness of human gut microbiome correlates with metabolic markers. *Nature 2013 500:7464* **500**, 541–546 (2013).
93. Turnbaugh, P. J. *et al.* An obesity-associated gut microbiome with increased capacity for energy harvest. *Nature* **444**, 1027–1031 (2006).
94. Ley, R. E. *et al.* Obesity alters gut microbial ecology. *Proc Natl Acad Sci U S A* **102**, 11070–11075 (2005).
95. Ley, R. E., Turnbaugh, P. J., Klein, S. & Gordon, J. I. Human gut microbes associated with obesity. *Nature 2006 444:7122* **444**, 1022–1023 (2006).
96. Kasai, C. *et al.* Comparison of the gut microbiota composition between obese and non-obese individuals in a Japanese population, as analyzed by terminal restriction fragment length polymorphism and next-generation sequencing. *BMC Gastroenterol* **15**, (2015).
97. Cani, P. D. *et al.* Metabolic endotoxemia initiates obesity and insulin resistance. *Diabetes* **56**, 1761–1772 (2007).
98. Bailey, M. T. *et al.* Exposure to a social stressor alters the structure of the intestinal microbiota: implications for stressor-induced immunomodulation. *Brain Behav Immun* **25**, 397–407 (2011).
99. Lyte, M., Vulchanova, L. & Brown, D. R. Stress at the intestinal surface: catecholamines and mucosa-bacteria interactions. *Cell Tissue Res* **343**, 23–32 (2011).
100. Collins, S. M., Surette, M. & Bercik, P. The interplay between the intestinal microbiota and the brain. *Nature Reviews Microbiology 2012 10:11* **10**, 735–742 (2012).
101. Carson, T. L. *et al.* Associations Between Race, Perceived Psychological Stress, and the Gut Microbiota in a Sample of Generally Healthy Black and White Women: A Pilot Study on the Role of Race and Perceived Psychological Stress. *Psychosom Med* **80**, 640–648 (2018).

102. Callaghan, B. L. *et al.* Mind and gut: Associations between mood and gastrointestinal distress in children exposed to adversity. *Dev Psychopathol* **32**, 309–328 (2020).
103. Hantsoo, L. *et al.* Childhood adversity impact on gut microbiota and inflammatory response to stress during pregnancy. *Brain Behav Immun* **75**, 240–250 (2019).
104. Aatsinki, A. K. *et al.* Maternal prenatal psychological distress and hair cortisol levels associate with infant fecal microbiota composition at 2.5 months of age. *Psychoneuroendocrinology* **119**, (2020).
105. Hantsoo, L. & Zemel, B. S. Stress Gets into the Belly: Early Life Stress and the Gut Microbiome HHS Public Access. *Behav Brain Res* **414**, 113474 (2021).
106. Ramirez, J. *et al.* Antibiotics as Major Disruptors of Gut Microbiota. *Front Cell Infect Microbiol* **10**, (2020).
107. Lange, K., Buerger, M., Stallmach, A. & Bruns, T. Effects of Antibiotics on Gut Microbiota. *Dig Dis* **34**, 260–268 (2016).
108. Palleja, A. *et al.* Recovery of gut microbiota of healthy adults following antibiotic exposure. *Nat Microbiol* **3**, 1255–1265 (2018).
109. Kumari, R. *et al.* Emerging frontiers of antibiotics use and their impacts on the human gut microbiome. *Microbiol Res* **263**, (2022).
110. Rogers, M. A. M. & Aronoff, D. M. The influence of non-steroidal anti-inflammatory drugs on the gut microbiome. *Clinical Microbiology and Infection* **22**, 178.e1-178.e9 (2016).
111. Di Tommaso, N., Gasbarrini, A. & Ponziani, F. R. Intestinal barrier in human health and disease. *Int J Environ Res Public Health* **18**, (2021).
112. Aydin, C. *et al.* Relaxant effect of omeprazole and lansoprazole in guinea pig gallbladder muscle strips in vitro. *J Gastroenterol* **38**, 765–771 (2003).
113. Li, Z., Summanen, P. H., Komoriya, T. & Finegold, S. M. In vitro study of the prebiotic xylooligosaccharide (XOS) on the growth of Bifidobacterium spp and Lactobacillus spp. *Int J Food Sci Nutr* **66**, 919–922 (2015).
114. Yang, J. *et al.* Xylooligosaccharide supplementation alters gut bacteria in both healthy and prediabetic adults: A pilot study. *Front Physiol* **6**, (2015).
115. Fei, Y. *et al.* Xylooligosaccharide Modulates Gut Microbiota and Alleviates Colonic Inflammation Caused by High Fat Diet Induced Obesity. *Front Physiol* **10**, (2020).

116. Florent, C. *et al.* Influence of chronic lactulose ingestion on the colonic metabolism of lactulose in man (an in vivo study). *Journal of Clinical Investigation* **75**, 608 (1985).
117. Clausen, M. R. & Mortensen, P. B. Lactulose, Disaccharides and Colonic Flora. Clinical consequences. *Drugs* **53**, 930–942 (1997).
118. Wang, S. P. *et al.* Pivotal Roles for pH, Lactate, and Lactate-Utilizing Bacteria in the Stability of a Human Colonic Microbial Ecosystem. *mSystems* **5**, (2020).
119. Reichardt, N. *et al.* Specific substrate-driven changes in human faecal microbiota composition contrast with functional redundancy in short-chain fatty acid production. *ISME J* **12**, 610–622 (2018).
120. Gibson, G. R., McCartney, A. L. & Rastall, R. A. Prebiotics and resistance to gastrointestinal infections. *British Journal of Nutrition* **93**, S31–S34 (2005).
121. Scholz-Ahrens, K. E. *et al.* Prebiotics, Probiotics, and Synbiotics Affect Mineral Absorption, Bone Mineral Content, and Bone Structure. *J Nutr* **137**, 838S-846S (2007).
122. Chu, N., Ling, J., Jie, H., Leung, K. & Poon, E. The potential role of lactulose pharmacotherapy in the treatment and prevention of diabetes. *Front Endocrinol (Lausanne)* **13**, (2022).
123. Schönfeld, P. & Wojtczak, L. Short- and medium-chain fatty acids in energy metabolism: the cellular perspective. *J Lipid Res* **57**, 943–954 (2016).
124. Mooranian, A. *et al.* Modulatory Nano/Micro Effects of Diabetes Development on Pharmacology of Primary and Secondary Bile Acids Concentrations. *Curr Diabetes Rev* **16**, 900–909 (2020).
125. Mooranian, A. *et al.* Pharmacological effects of nanoencapsulation of human-based dosing of probucol on ratio of secondary to primary bile acids in gut, during induction and progression of type 1 diabetes. *Artif Cells Nanomed Biotechnol* **46**, S748–S754 (2018).
126. Pandey, Kavita. R., Naik, Suresh. R. & Vakil, Babu. v. Probiotics, prebiotics and synbiotics- a review. *J Food Sci Technol* **52**, 7577–7587 (2015).
127. Gibson, G. R. *et al.* Expert consensus document: The International Scientific Association for Probiotics and Prebiotics (ISAPP) consensus statement on the definition and scope of prebiotics. *Nat Rev Gastroenterol Hepatol* **14**, 491–502 (2017).

128. Swanson, K. S. *et al.* The International Scientific Association for Probiotics and Prebiotics (ISAPP) consensus statement on the definition and scope of synbiotics. *Nat Rev Gastroenterol Hepatol* **17**, 687–701 (2020).
129. Yadav, M. K., Kumari, I., Singh, B., Sharma, K. K. & Tiwari, S. K. Probiotics, prebiotics and synbiotics: Safe options for next-generation therapeutics. *Appl Microbiol Biotechnol* **106**, 505–521 (2022).
130. Soleimani, A. *et al.* The Effects of Synbiotic Supplementation on Metabolic Status in Diabetic Patients Undergoing Hemodialysis: a Randomized, Double-Blinded, Placebo-Controlled Trial. *Probiotics Antimicrob Proteins* **11**, 1248–1256 (2019).
131. Wagner, M. Single-Cell Ecophysiology of Microbes as Revealed by Raman Microspectroscopy or Secondary Ion Mass Spectrometry Imaging. *Annu Rev Microbiol* **63**, 411–429 (2009).
132. Berry, D. *et al.* Tracking heavy water (D2O) incorporation for identifying and sorting active microbial cells. *Proc Natl Acad Sci U S A* **112**, E194–E203 (2015).
133. Lee, K. S. *et al.* An automated Raman-based platform for the sorting of live cells by functional properties. *Nat Microbiol* **4**, 1035–1048 (2019).
134. Aida Kadunic. Evaluating the selectivity of prebiotics lactulose and xylooligosaccharides (XOS) in human gut microbiota. (University of Vienna , 2019).
135. Wright, E. S. Using DECIPHER v2.0 to Analyze Big Biological Sequence Data in R. *The R Journal* **8**, (2016).
136. Altschul, S. F., Gish, W., Miller, W., Myers, E. W. & Lipman, D. J. Basic local alignment search tool. *J Mol Biol* **215**, 403–410 (1990).
137. Pruesse, E., Peplies, J. & Glöckner, F. O. SINA: Accurate high-throughput multiple sequence alignment of ribosomal RNA genes. *Bioinformatics* **28**, 1823–1829 (2012).
138. Yilmaz, P. *et al.* The SILVA and “All-species Living Tree Project (LTP)” taxonomic frameworks. *Nucleic Acids Res* **42**, D643–D648 (2014).
139. Quast, C. *et al.* The SILVA ribosomal RNA gene database project: Improved data processing and web-based tools. *Nucleic Acids Res* **41**, (2013).
140. Nguyen, L. T., Schmidt, H. A., von Haeseler, A. & Minh, B. Q. IQ-TREE: A fast and effective stochastic algorithm for estimating maximum-likelihood phylogenies. *Mol Biol Evol* **32**, 268–274 (2015).

141. Letunic, I. & Bork, P. Interactive tree of life (iTOL) v5: An online tool for phylogenetic tree display and annotation. *Nucleic Acids Res* **49**, W293–W296 (2021).
142. Okazaki, M., Fujikawa, S. & Matsumoto, N. Effect of Xylooligosaccharide on the Growth of Bifidobacteria. *Bifidobacteria and Microflora* **9**, 77–86 (1990).
143. Campbell, J. M., Fahey, G. C. & Wolf, B. W. Selected indigestible oligosaccharides affect large bowel mass, cecal and fecal short-chain fatty acids, pH and microflora in rats. *J Nutr* **127**, 130–136 (1997).
144. Hsu, C. K., Liao, J. W., Chung, Y. C., Hsieh, C. P. & Chan, Y. C. Xylooligosaccharides and fructooligosaccharides affect the intestinal microbiota and precancerous colonic lesion development in rats. *J Nutr* **134**, 1523–1528 (2004).
145. Gobinath, D., Madhu, A. N., Prashant, G., Srinivasan, K. & Prapulla, S. G. Beneficial effect of xylo-oligosaccharides and fructo-oligosaccharides in streptozotocin-induced diabetic rats. *British Journal of Nutrition* **104**, 40–47 (2010).
146. Rycroft, C. E., Jones, M. R., Gibson, G. R. & Rastall, R. A. A comparative in vitro evaluation of the fermentation properties of prebiotic oligosaccharides. *J Appl Microbiol* **91**, 878–887 (2001).
147. Crittenden, R. *et al.* In vitro fermentation of cereal dietary fibre carbohydrates by probiotic and intestinal bacteria. *J Sci Food Agric* **82**, 781–789 (2002).
148. Sun, Z., Yue, Z., Liu, E., Li, X. & Li, C. Assessment of the bifidogenic and antibacterial activities of xylooligosaccharide. *Front Nutr* **9**, (2022).
149. Hidalgo-Cantabrana, C. *et al.* Bifidobacteria and Their Health-Promoting Effects. *Microbiol Spectr* **5**, (2017).
150. Delgado, S., Suárez, A. & Mayo, B. Bifidobacterial diversity determined by culturing and by 16S rDNA sequence analysis in feces and mucosa from ten healthy spanish adults. *Dig Dis Sci* **51**, 1878–1885 (2006).
151. Turroni, F. *et al.* Exploring the diversity of the bifidobacterial population in the human intestinal tract. *Appl Environ Microbiol* **75**, 1534–1545 (2009).
152. Monteagudo-Mera, A. *et al.* High purity galacto-oligosaccharides enhance specific Bifidobacterium species and their metabolic activity in the mouse gut microbiome. *Benef Microbes* **7**, 247–264 (2016).

153. Tamotsu, K. *et al.* Multiple Omics Uncovers Host–Gut Microbial Mutualism During Prebiotic Fructooligosaccharide Supplementation. *DNA Research* **21**, 469–480 (2014).
154. Jung, T. H., Jeon, W. M. & Han, K. S. In Vitro Effects of Dietary Inulin on Human Fecal Microbiota and Butyrate Production. *J. Microbiol. Biotechnol.* **25**, 1555–1558 (2015).
155. Yang, J. *et al.* Combining of transcriptome and metabolome analyses for understanding the utilization and metabolic pathways of Xylo-oligosaccharide in Bifidobacterium adolescentis ATCC 15703. *Food Sci Nutr* **7**, 3480 (2019).
156. Mao, B. *et al.* In vitro fermentation of lactulose by human gut bacteria. *J Agric Food Chem* **62**, 10970–10977 (2014).
157. Cui, S. *et al.* Lactulose significantly increased the relative abundance of *Bifidobacterium* and *Blautia* in mice feces as revealed by 16S rRNA amplicon sequencing. *J Sci Food Agric* **101**, 5721–5729 (2021).
158. Cronin, M., Ventura, M., Fitzgerald, G. F. & van Sinderen, D. Progress in genomics, metabolism and biotechnology of bifidobacteria. *Int J Food Microbiol* **149**, 4–18 (2011).
159. Lee, J.-H. & O'Sullivan, D. J. Genomic Insights into Bifidobacteria. *Microbiology and Molecular Biology Reviews* **74**, 378–416 (2010).
160. Kassinen, A. *et al.* The Fecal Microbiota of Irritable Bowel Syndrome Patients Differs Significantly From That of Healthy Subjects. *Gastroenterology* **133**, 24–33 (2007).
161. Shapiro, J. *et al.* Psoriatic patients have a distinct structural and functional fecal microbiota compared with controls. *J Dermatol* **46**, 595–603 (2019).
162. Clavel, T., Lepage, P. & Charrier, C. The Family Coriobacteriaceae. in *The Prokaryotes* 201–238 (Springer Berlin Heidelberg, 2014). doi:10.1007/978-3-642-30138-4_343.
163. Song, A. A.-L., In, L. L. A., Lim, S. H. E. & Rahim, R. A. A review on Lactococcus lactis: from food to factory. *Microb Cell Fact* **16**, 55 (2017).
164. Kontula, P., Suihko, M.-L., von Wright, A. & Mattila-Sandholm, T. The Effect of Lactose Derivatives on Intestinal Lactic Acid Bacteria. *J Dairy Sci* **82**, 249–256 (1999).

165. Khemariya, P., Singh, S., Nath, G. & Gulati, A. K. Probiotic Lactococcus lactis: A Review. *Turkish Journal of Agriculture - Food Science and Technology* **5**, 556 (2017).
166. Finegold, S. M. *et al.* Xylooligosaccharide increases bifidobacteria but not lactobacilli in human gut microbiota. *Food Funct* **5**, 436–445 (2014).
167. Chen, Y. *et al.* Xylo-Oligosaccharides, Preparation and Application to Human and Animal Health: A Review. *Front Nutr* **8**, (2021).
168. Samanta, A. K. *et al.* Xylooligosaccharides as prebiotics from agricultural by-products: Production and applications. *Bioactive Carbohydrates and Dietary Fibre* **5**, 62–71 (2015).